(12) INTERNATIONAL APPLICATION PUBLISHED UNDER THE PATENT COOPERATION TREATY (PCT)

(19) World Intellectual Property Organization
International Bureau

(43) International Publication Date
14 November 2002 (14.11.2002)

PCT

(10) International Publication Number
WO 02/091353 A1

(51) International Patent Classification[7]: G10K 11/178

(21) International Application Number: PCT/NL02/00297

(22) International Filing Date: 6 May 2002 (06.05.2002)

(25) Filing Language: English

(26) Publication Language: English

(30) Priority Data:
1018014 7 May 2001 (07.05.2001) NL

(71) Applicant *(for all designated States except US)*: **NEDERLANDSE ORGANISATIE VOOR TOEGEPAST-NATUURWETENSCHAPPELIJK ONDERZOEK TNO** [NL/NL]; Schoemakersstraat 97, NL-2628 VK Delft (NL).

(72) Inventor; and

(75) Inventor/Applicant *(for US only)*: **BERKHOFF, Arthur, Perry** [NL/NL]; Prins Hendrikplein 6, NL-2518 JA Den Haag (NL).

(74) Agent: **PRINS, A., W.**; Vereenigde, Nieuwe Parklaan 97, NL-2587 BN The Hague (NL).

(81) Designated States *(national)*: AE, AG, AL, AM, AT (utility model), AT, AU, AZ, BA, BB, BG, BR, BY, BZ, CA, CH, CN, CO, CR, CU, CZ (utility model), CZ, DE (utility model), DE, DK (utility model), DK, DM, DZ, EC, EE (utility model), EE, ES, FI (utility model), FI, GB, GD, GE, GH, GM, HR, HU, ID, IL, IN, IS, JP, KE, KG, KP, KR, KZ, LC, LK, LR, LS, LT, LU, LV, MA, MD, MG, MK, MN, MW, MX, MZ, NO, NZ, OM, PH, PL, PT, RO, RU, SD, SE, SG, SI, SK (utility model), SK, SL, TJ, TM, TN, TR, TT, TZ, UA, UG, US, UZ, VN, YU, ZA, ZM, ZW.

[Continued on next page]

(54) Title: ANTI NOISE SYSTEM AND METHOD USING BROADBAND RADIATION MODES

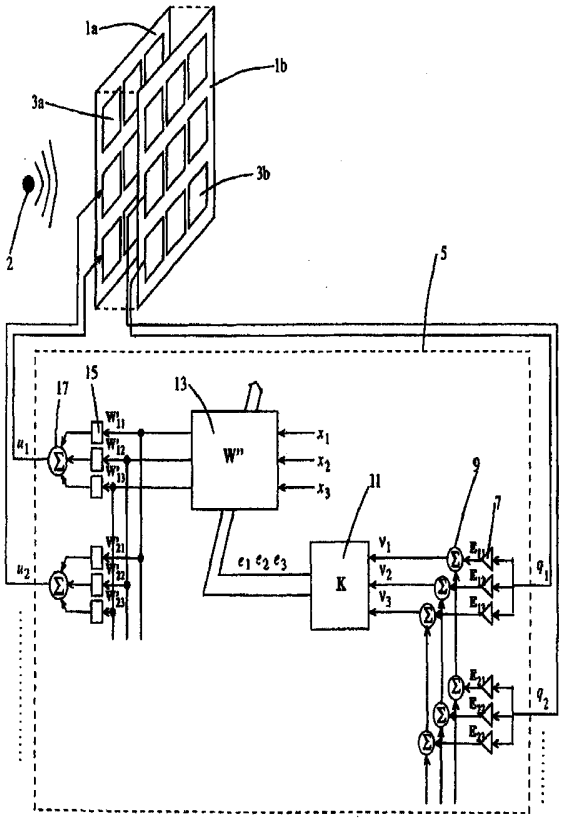

(57) Abstract: Anti noise system and method, in particular for suppressing sound radiated from a structure, using a formulation of the most efficiently radiating vibration patterns of a vibrating body, the radiation modes, in the time domain. The radiation modes can be used to arrive at efficient weighting schemes for an array of sensors in order to reduce controller dimensionality. The particular radiation modes are determined on the basis of broadband signals. A method is given to obtain these modes from measurable signals on nearfield sensors and microphones in the farfield. The broadband radiation modes are used for the design of an actuator array in a feedback control system to reduce sound power radiated from an object. Three different methods for the design of the actuator are compared, taking into account the reduction of radiated sound power in the controlled frequency range, but also a possible increase of radiated sound power in an uncontrolled frequency range.

WO 02/091353 A1

(84) Designated States *(regional)*: ARIPO patent (GH, GM, KE, LS, MW, MZ, SD, SL, SZ, TZ, UG, ZM, ZW), Eurasian patent (AM, AZ, BY, KG, KZ, MD, RU, TJ, TM), European patent (AT, BE, CH, CY, DE, DK, ES, FI, FR, GB, GR, IE, IT, LU, MC, NL, PT, SE, TR), OAPI patent (BF, BJ, CF, CG, CI, CM, GA, GN, GQ, GW, ML, MR, NE, SN, TD, TG).

Published:

— *with international search report*

— *before the expiration of the time limit for amending the claims and to be republished in the event of receipt of amendments*

For two-letter codes and other abbreviations, refer to the "Guidance Notes on Codes and Abbreviations" appearing at the beginning of each regular issue of the PCT Gazette.

Title: Anti noise system and method using broadband radiation modes

The present invention relates to an anti noise system for suppressing primary signals in a space due to a primary source, such as sound radiated from a structure. More particularly the invention relates to a system comprising:

- one or more secondary sources to produce secondary signals to suppress the primary signals in the space;
- one or more sensors to produce sensor output signals in relation to the secondary sources;
- a controller arranged to:
  - receive the sensor output signals;
  - calculate error signals by weighting the sensor output signals with radiation mode shapes determined for at least one predetermined frequency;
  - use the error signals to control an adaptive filter to produce drive signals for the secondary sources.

Active control of sound radiated from structures using structural sensing involves controlling the vibration patterns of the structure that radiate sound efficiently. Several methods have been suggested to determine these vibration patterns. The methods can be based on the singular value decomposition of the Green's function [1, 2] or an eigenvector analysis of a positive definite radiation operator [3]. The resulting vibration patterns are called radiation mode shapes [2, 4]. The associated singular values/eigenvalues can be interpreted as radiation efficiencies. Borgiotti [1] noted that the radiation modes are real valued and therefore, in principle, allow delay-free sensing of acoustic radiation. A sensor without delay is particularly important in feedback configurations.

A complication for a real-time implementation is that both the radiation mode shapes as well as the radiation efficiencies depend on frequency. A solution was given later by Borgiotti and Jones [5] who

demonstrated that minimizing the radiation modal error signals, that are obtained by weighting the sensor signals with the radiation mode shapes at the highest controlled frequency, is sufficient to reduce the sound also at lower frequencies. This is because the radiation modes at a certain frequency form a complete description of the radiating vibration patterns at lower frequencies. Thus, a single set of radiation mode shapes is used for all frequencies, although these radiation mode shapes have been obtained for a single frequency (the highest controlled frequency, or, as it will be called in the following the normalization frequency).

At frequencies other than the frequency where the radiation modes have been determined, the so-called normalization frequency [6], the radiation modes do not diagonalize the radiation operator, except for special cases [7]. Therefore, in principle, if the radiation modes at a single normalization frequency are used, all self radiation efficiencies and mutual radiation efficiencies have to be taken into account to be able to compute the exact radiated power at other frequencies. Simplifications were given [8, 9], demonstrating that good sound power reductions can be obtained by using only the self radiation efficiencies. It was also shown that the choice of the radiation mode shapes is not critical, provided they form a complete set of basis functions for the radiating vibration patterns in the frequency range of interest [9]. In some cases, such as for free-field sound radiation, frequency dependent weighting might not be strictly necessary [9]. In other cases, however, a frequency dependent weighting of the radiation modal error signals was found to be necessary, especially in enclosed spaces [10]. There seems to be agreement that frequency independent spatial filters can, in general, be used for broadband active noise control problems involving sound radiation from plates.

Even if a frequency dependent weighting of the radiation modal error signals is used, still a choice has to be made which normalization frequency to use. Moreover, in many practical situations, calculations based on

theoretical simplifications, e.g., starting with flat vibrating plates (e.g., done by Gibbs, et al. [8]), do not render optimum results.

Summary of the invention

It is therefore an object of the present invention to provide an anti noise system that provides improved anti noise control in practical situations, e.g. situations where vibrating bodies do not have a theoretically simple shape or are present in enclosed volumes of complex form and materials. To that end, an anti noise system according to the invention as defined in the preamble is characterized in that the controller is also arranged to

- calculate the error signals by weighting the sensor output signals with radiation mode shapes determined for a plurality of frequencies in a predetermined frequency band.

Thus, the invention addresses the determination of the radiation mode shapes and associated efficiencies based on broadband sound radiation. In contrast to the prior art solutions, the system does not determine the radiation mode shapes for transfer characteristics obtained from measurements for a single normalization frequency. Instead the system uses determines the radiation mode shapes for what is effectively a frequency averaged transfer characteristic. As shown in appendix A, this ensures a complete set of modes. The radiation modes obtained in this way are the optimum vibration patterns in an average sense evaluated over a predefined frequency band. This eliminates the need for selection of a normalization frequency.

Subsequent frequency dependent weighting can be obtained by evaluating the self and mutual radiation efficiencies of the resulting radiation modes. Instead of using a frequency domain formulation, a time domain formulation to determine the radiation modes is proposed. That is, no explicit averaging over frequencies is needed. This leads to advantages for the

identification of radiation modes from experimental data, in which robustness is a primary concern. Preumont et al. [11] determined weighting coefficients for a piezoelectric sensor array for the estimation of the volume velocity, which is the strongest radiation mode at low frequencies. One of the possible extensions of the present invention is that it also leads to weighting factors for higher-order radiation modes. Another possible extension is that the radiation modes can be determined from pressure measurements in the far field instead of using a particular velocity distribution (viz. constant velocity) and assuming that this velocity distribution is responsible for the major part of the radiated acoustic power. Also in the work of Gibbs et al. [8] a theoretical model is used for the radiation into the acoustic environment.

In a preferred embodiment, the weighting schemes for the actuator array are optimized in a broadband sense for coupling to the acoustic field at low frequencies, while being constrained by a reduced coupling to the acoustic field at high frequencies. This minimizes the 'spillover' effect [12], which can lead to undesirable increases in sound power of the high frequency components if the low 30 frequency components are reduced.

Modal sensors and modal actuators based on spatially continuous transducers were discussed by Lee and Moon [13]. The invention is preferably based on discrete sensors and actuators, such as described by Gawronski [14] and Morgan [15], in order to provide more flexibility by using programmable weighting coefficients. The emphasis in the present invention is on acoustic radiation and the connection with previous radiation mode theory.

The present invention also relates to an anti noise method for suppressing primary signals in a space due to a primary source, comprising the steps of:

- producing secondary signals by one or more secondary sources to suppress the primary signals in the space;
- producing sensor output signals in relation to the secondary sources by one or more sensors;

- performing the following steps by a controller:
  - receiving the sensor output signals;
  - calculating error signals by weighting the sensor output signals with radiation mode shapes determined for at least one predetermined frequency;
  - using the error signals to control an adaptive filter to produce drive signals for the secondary sources;

wherein the method also performs the following step by the controller:
  - calculating the error signals by weighting the sensor output signals with radiation mode shapes determined for a plurality of frequencies in a predetermined frequency band.

Moreover, the invention relates to a computer program product to be loaded by an anti noise system for suppressing primary signals in a space due to a primary source, the system comprising:
- one or more secondary sources to produce secondary signals to suppress the primary signals in the space;
- one or more sensors to produce sensor output signals in relation to the secondary sources;
- a controller;

the computer program product, after being loaded, providing the controller of the anti noise system with the capacity to:
- receive the sensor output signals;
- calculate error signals by weighting the sensor output signals with radiation mode shapes determined for at least one predetermined frequency;
- use the error signals to control an adaptive filter to produce drive signals for the secondary sources;

wherein the computer program product, after being loaded, provides the controller also with the capacity to:

- calculate the error signals by weighting the sensor output signals with radiation mode shapes determined for a plurality of frequencies in a predetermined frequency band.

In a further alternative, the present invention relates to a data carrier provided with a computer program product, as defined above.

The invention also relates to a method for identification of multiple radiation modes from experimental data by using further sensors, e.g., microphones, in the far field, the far field being defined as comprising those locations which are further away from the secondary sources than the longest wave length of interest. To that end the present invention provides a method of calibrating an anti noise system as defined above, comprising the steps of:

- driving the one or more secondary sources with a plurality of different excitation patterns;
- producing further sensor output signals by measuring signals in the space due to the plurality of different excitation patterns with further sensors in the space;
- applying the sensor output signals and the further sensor output signals to the controller;
- using a time-domain inverse filtering technique by the controller to determine the radiation mode shapes and radiation efficiencies.

However, the calibration can also be done in an alternative way. To that end, the invention also relates to a method of calibrating an anti noise system as defined above, comprising the steps of:

- driving one or more volume velocity sources with a known volume velocity in predetermined locations remote from the secondary sources;
- measuring pressure signals due to the volume velocity sources with sensors on a structure supporting the secondary sources;

- applying the value of the volume velocity and the pressure signals to the controller;
- determining the radiation mode shapes.

The calibration can also be done in a further alternative way. To that end, the invention also relates to a method of calibrating an anti noise system as defined above, comprising the steps of:

- driving one or more secondary sources with a plurality of different excitation patterns and measuring the sensor output signals;
- applying the excitation patterns and the sensor output signals to the controller;
- driving one or more sources with a known volume velocity in a predetermined location remote from the secondary sources and measuring output signals of the secondary sources due to these sources;
- applying the value of the volume velocity and the output signals on the secondary sources to the controller;
- using a time-domain inverse filtering technique by the controller to determine the radiation mode shapes.

Brief description of the drawings

The invention will be explained in detail with reference to some drawings which are only intended for illustration purposes and not to limit the scope of the invention as defined by the accompanying claims.

Figure 1 shows a transfer function from actuator current to far field pressure
Figures 2a, 2b, 2c, 2d show the radiation mode shapes
Figure 3 shows eigenvalues obtained with a time domain technique
Figures 4a, 4b, 4c, 4d show radiation mode shapes

Figure 5 shows eigenvalues obtained with a frequency domain technique

Figures 6a, 6b, 6c, 6d, show radiation mode shapes

Figure 7 shows eigenvalues

Figures 8a, 8b, 8c, 8d, show radiation mode shapes

Figure 9 shows eigenvalues obtained with the reconstructed Green's function.

Figure 10 shows a schematic diagram of an active feedback control system

Figure 11a shows a configuration for calibration of the system

Figure 11b shows a configuration for the reduction of sound

Figure 12 shows an actuator configuration and a sensor configuration

Figure 13 shows the sound transmitted with and without feedback control,

Figure 11b shows a configuration for the reduction of sound transmitted through a plate by using weighting schemes for actuators and sensors. A primary sound field is due to a source 2 which produces primary vibrations of a structure 1a, 1b. Although the primary source (2) as indicated in Figure 11b is an acoustic source, the actual primary source can also be a mechanical primary source which directly excites the structure.

Figure 11b shows an object or structure 1a, 1b e.g., a plate (that may have an arbitrary shape and may be located in an enclosure), that is made to vibrate by means of a plurality of actuators 3a. The actuators 3a may be piezo-electric transducers or shakers driven by a driving signal **u**. Object 1 also contains a plurality of sensors 3b. In a preferred embodiment the sensors 3b consist of piezoelectric transducers and may be combined with the actuators 3a into the same physical transducers. Each of the sensors 3b produce an output signal corresponding with quantity **q** (e.g. velocity or pressure or strain). The output signals **q** are received by a controller 5.

The controller 5 comprises means for multiplying the output signals **q** by the radiation modes **E**. The resulting signals are summed to render error signals **v**. Block 11 denotes that the controller 5 is arranged with means to (optionally) perform a frequency dependent weighting operation **K** on error

signals **v** to provide resulting error signals **e** (equation (20)). The resulting error signals e are used by the controller 5 to control adaptive parameters of an adaptive controller 13. Adaptive controller 13 produces output signals applied to a filter 15 with fixed filter coefficients **W'**. Filter 15 produces actuator drive signals **u**. These actuator drive signals **u** are optionally amplified.

The controller 5 has been shown in a very schematic way to clearly demonstrate the different signals of the calculations presented here. The blocks shown in controller 5 need not be physically present. There may be just one processor performing all the necessary calculations and simulating the block scheme of figure 11b . Alternatively, the controller may be designed with different parallel operating processors or with processors in a master-slave configuration, as is known to persons skilled in the art. Basically, there is no restriction as to how the controller is designed as long as it is capable of performing the essential features of the annexed claims. Even analoque and/or digital circuits can be used, as the case may be.

Figure 11a shows a configuration for calibration of the system, that is the determination of coefficients involved in the weighting operation K, the filter coefficients W', W" and/or the radiation modes E. The calibration procedure uses excitation of the structure 1 and the simultaneous measurement of the sensor output signals **q** and the corresponding far field pressure signals **p**.

The radiation modes **E** are identified in situ. The method of identifying the radiation modes is based on the excitation of the structure with a number of different excitation patterns and acquisition of the resulting structural sensor signals **q** and far field pressure signals **p** with the configuration shown in Figure 11a. A time-domain inverse filtering technique is used to extract an underlying Green's function, which gives the response in the far field in terms of elementary sources on the structure. The time domain

technique has the advantage that a single minimization procedure is used to obtain the complete impulse response.

This should be contrasted with frequency domain techniques, for which the impulse response has to be assembled from partial optimization results, each using a limited information content. This makes the frequency domain technique potentially less robust because if the inversion fails for one of the frequency components which constitute the impulse response, the whole impulse response could be rendered useless. This is a problem particularly where the excited structure has strong resonating behavior, such as with vibrating plates. Also an averaging procedure over different frequencies would not be a real improvement because it is still based on unreliable constituents.

The theoretical basis of the calibration process will be explained in more detail in the following.

1 Radiation modes for sensor arrays; theory

The acoustic power radiated from a vibrating structure to the far field can be derived from measurement of the time-averaged squared sound pressure at a relatively large distance from the structure using a sufficient number of measurement positions [16]. Global sound pressure reduction inside an enclosure is related to the reduction of the potential energy in the enclosure, which can be estimated from the squared sound pressure at a number of positions (N) evenly distributed over the interior of the enclosure. Thus for some interesting problems involving sound radiation it seems appropriate to define a cost function

$$\Pi = E\{\mathbf{p}^T(t)\mathbf{p}(t)\} \tag{1}$$

with

$$\mathbf{p}(t) = [p_1(t)\ p_2(t)\ \ldots p_N(t)]^T \tag{2}$$

the N x 1 dimensional vector of pressure signals at discrete time t and E the expected value operator, which, for a time dependent matrix $\mathbf{F}(t)$, is defined as

$$E\{\mathbf{F}(t)\} = \lim_{T\to\infty} \frac{1}{T} \sum_{t=0}^{T-1} \mathbf{F}(t) \tag{3}$$

The pressure $p_n(t)$, $n = 1, \ldots, N$ at position n is assumed to be related to the vibrations of the structure (which can be velocity or strain or another quantity) through the relationship

$$p_n(t) = \sum_{m=1}^{M} \sum_{r=0}^{T-1} g_{mn}(\tau) q_m(t-\tau) \tag{4}$$

where $q_m(t)$ is the m-th sensed quantity on the structure and where $g_{mn}(t)$ is the space-time Green's function for the problem. Further, T denotes the number of samples taken into account, i.e. the length of the impulse response of $g_{mn}(t)$. It is noted that in many definitions of Green's functions for problems in acoustics an additional temporal differentiation has to be applied, such as for the Rayleigh integral [16]. However, here the additional differentiation and other temporal characteristics are incorporated in $g_{mn}(t)$.

Let us define the M x 1 dimensional vectors

$$\mathbf{g}_n(t) = [g_{1n}(t)\ g2n(t) \ldots g_{Mn}(t)]^T, \quad n = 1, \ldots, N, \tag{5}$$

and the N x M dimensional matrix

$$\mathbf{G}(t) = [\mathbf{g}_1(t)\ \mathbf{g}_2(t) \ldots \mathbf{g}_N(t)]^T \tag{6}$$

Further let us define an M x 1 dimensional structural sensor vector as

$$\mathbf{q}(t) = [q_1(t)\ q_2(t)\ \ldots\ q_M(t)]^T \tag{7}$$

We then have

$$\mathbf{p}(t) = \sum_{\tau=0}^{T-1} \mathbf{G}(\tau)\mathbf{q}(t-\tau) \tag{8}$$

Using Eq. (1), this leads to the expression

$$\Pi = E\left\{\sum_{\tau=0}^{T-1}\sum_{\tau'=0}^{T-1} q^T(t-\tau')\mathbf{G}^T(\tau')\mathbf{G}(\tau)\mathbf{q}(t-\tau)\right\} \tag{9}$$

It can be seen that the relation between $\mathbf{q}(t)$ and Π is determined by the kernel $\mathbf{G}^T(\tau')\mathbf{G}(\tau)$. For reasons of convenience, we turn to a frequency domain description where all variables now depend on angular frequency ω and are complex valued. In this decription, the frequency domain equivalents of corresponding temporal variables are indicated by adding a hat sign. A discrete-time Fourier transform pair for matrices $\mathbf{P}(t)$ and $\hat{\mathbf{P}}(\omega)$ is defined as [17, 18]:

$$\hat{\mathbf{P}}(\omega) = \sum_{t=-\infty}^{\infty} \mathbf{P}(t)_e\ -i\omega t/f_s \tag{10}$$

$$\mathbf{P}(t) = \frac{1}{2\pi f_s}\int_{-\pi f_s}^{\pi f_d} \hat{\mathbf{P}}(\omega)e^{i\omega t/f_s}d\omega \tag{11}$$

with ω the angular frequency in rad/s and f_s the sampling frequency in Hz.

At each angular frequency, the cost function can be expressed as:

$$\hat{\Pi}(\omega) = \hat{\mathbf{p}}^H(\omega)\hat{\mathbf{p}}(\omega) \tag{12}$$

where a superscripted *H* denotes the Hermitian transpose. Using the frequency domain equivalent of Eq. (8), viz.

$$\hat{\mathbf{p}}(\omega) = \hat{\mathbf{G}}(\omega)\hat{\mathbf{q}}(\omega) \tag{13}$$

the cost function becomes

$$\hat{\Pi}(\omega) = \hat{\mathbf{q}}^{H}(\omega)\hat{\mathbf{P}}_{GG}(\omega)\hat{\mathbf{q}}(\omega) \tag{14}$$

where

$$\hat{\mathbf{P}}_{GG}(\omega) = \hat{\mathbf{G}}^{H}(\omega)\hat{\mathbf{G}}(\omega) \tag{15}$$

The M x M dimensional matrix $\hat{\mathbf{P}}_{GG}(\omega)$ contains information about the vibration patterns of $\hat{\mathbf{q}}(\omega)$ that are significant to $\hat{\mathbf{p}}(\omega)$. These vibration patterns can be obtained by an eigenvector analysis of $\hat{\mathbf{P}}_{GG}(\omega)$, which is a well-known procedure ([19], p.72). In the limit for an infinite number of pressure sensors at an infinite distance from the radiator, assuming that $\hat{\mathbf{q}}(\omega)$ represents a velocity vector, the matrix $\hat{\mathbf{P}}_{GG}(\omega)$ approaches the matrix $\mathbf{R}(\omega)$ of Elliott and Johnson [4] up to a scaling factor.

Use of Eq. (10) shows that a so-called transfer correlation matrix

$$\mathbf{P}_{GG}(\tau) = E\{\mathbf{G}^{T}(t)\mathbf{G}(t+\tau)\},\ \tau = -T+1, \ldots, T-1, \tag{16}$$

is the time domain equivalent of Eq. (15). It is noted that in these descriptions the order of the transpose operators and Hermitian operators are different from usual descriptions of spectral density matrices and corresponding correlation matrices, such as in [18, 20]. From Eq. (11) it can be seen that the value of $\mathbf{P}_{GG}(t)$ for $t = 0$ is proportional to the integral over ω of the spectral density matrix (of transfer functions), and thus a measure of signal power (transfer) in a broadband sense. The term signal power is used here because

the sum of squared pressures is not a power in a physical sense. The most efficiently radiating, zero-delay vibration patterns in a broadband sense result from the decomposition of the zero lag transfer correlation matrix:

$$\mathbf{P}_{GG}(0) = \mathbf{E}\Lambda\mathbf{E}^{T} \tag{17}$$

where the matrix $\mathbf{E}$, with coefficients $\mathbf{E}_{ml}$, contains the broadband radiation mode shapes and the diagonal matrix Λ contains the broadband radiation efficiencies. Since $\mathbf{P}_{GG}(0)$ is symmetric, positive definite and real, the eigenvalues are also real. The matrices $\mathbf{E}$ and Λ are truncated to retain only the most significant, principal, components. In theory, the radiation modes obtained from the integral of $\hat{\mathbf{P}}_{GG}(\omega)$ over ω are identical to that obtained from $\mathbf{P}_{GG}(0)$. However, in practice, there is an important difference if they are obtained from measured data, as will be made clear in the next section. Zero delay radiation modes for a certain frequency band can be obtained after bandpass filtering of the Green's functions that lead to $\mathbf{P}_{GG}(t)$.

Error signals $\mathbf{u}(t) = [u_1(t)\ u_2(t)\ \ldots\ u_L(t)]^T$ for active control can be obtained by weighting the structural sensor vector $\mathbf{q}(t)$ with the radiation mode shapes in $\mathbf{E}$:

$$\mathbf{u}(t) = \mathbf{E}^{T}\mathbf{q}(t), \tag{18}$$

with possible subsequent frequency dependent weighting by the matrix $\tilde{\Lambda}(\omega) = \mathbf{E}^{T}\hat{\mathbf{P}}_{GG}(\omega)\mathbf{E}$[9].. The corresponding frequency domain cost function becomes

$$\hat{\Pi}(\omega) = \hat{v}^{H}(\omega)\tilde{\Lambda}(\omega)\hat{v}(\omega) \tag{19}$$

The resulting error signal $\mathbf{e}(t) = [e_1(t)e_2(t)\ \ldots\ e_L(t)]^T$, which is obtained by a frequency dependent weighting of $\mathbf{u}(t)$, is expressed as:

$$\mathbf{e}(t) = \sum_{\tau=0}^{T-1} \mathbf{K}(\tau)\mathbf{v}(t-\tau) \tag{20}$$

where $\mathbf{K}(t)$ is implicitly defined by

$$\tilde{\Lambda}(\omega) = \sum_{\tau=-\infty}^{\infty} E\{\mathbf{K}^T(t)\mathbf{K}(t+\tau)\}e^{-i\omega\tau/f_s} \tag{21}$$

If the full matrix $\tilde{\Lambda}(\omega)$ is used then the exact matrix $\hat{\mathbf{P}}(\omega)$ and the corresponding correlation matrix of Eq. (16) are reconstructed. Methods to find $\mathbf{K}(t)$ from rational matrices $\tilde{\Lambda}(\omega)$ can be found in papers by, e.g., Youla [21]; methods with application to acoustic radiation problems are also known [22]. In many cases it will be sufficient in the present description to use only the diagonal of $\tilde{\Lambda}(\omega)$ or even no weighting at all. In the latter case, $\tilde{\Lambda}(\omega)$ equals the identity matrix.

The eigenvectors in E are not completely orthogonal for acoustic radiation at each frequency but only approximately. They are however usable for broadband sound radiation control in the same sense as the radiation modes at the highestcontrolled frequency, as suggested for free space radiation by Borgiotti and Jones [5]. The essential observation to be made is that, because the radiation modes at a certain highest frequency are a complete set of basis functions for acoustic radiation at all lower frequencies, then also the eigenvectors obtained from an averaging procedure over frequency up to this highest frequency, that lead to Eq. (17), are a complete set of basis functions. A proof is given in the appendix. Although the resulting eigenvectors are not radiating independently, and consequently are not modes in a strict sense, they are called broadband radiation modes because of the close correspondence with the frequency domain radiation modes.

Broadband radiation modes also provide an unambiguous solution to the selection of a set of basis functions in enclosed spaces. In enclosed spaces, Borgiotti and Jones' suggestion does not always give the best results because

of the strong frequency dependence of the radiation modes. If broadband radiation modes are used then automatically the modes are selected which are optimum for the frequency range of interest, because all frequency dependent radiation properties are taken into account. However, these modes are optimum in an average sense and a subsequent frequency dependent weighting may be required. Another property of the time domain technique is that the resulting radiation modes are real valued. For positive definite radiation operators, this also holds for frequency domain techniques but in practice, using measured data from a finite number of field sensors at a finite distance, these radiation modes are not entirely real.

2 Estimation of the Green's function

2.1 Inverse method

The formulation of the previous section can be used for the identification of the radiation modes **E** in situ. The method is based on the excitation of the structure with a number of different excitation patterns and acquisition of the resulting structural sensor signals **q** and far field pressure signals **p**. The configuration is shown in Figure 11a. A time-domain inverse filtering technique is used to extract the underlying Green's function, which gives the response in the far field in terms of elementary sources on the structure. The time domain technique has the advantage that a single minimization procedure is used to obtain the complete impulse response. Instead, for the frequency domain technique, the impulse response has to be assembled from partial optimization results, each using a limited information content. This makes the frequency domain technique potentially less robust because if the inversion fails for one of the frequency components which constitute the impulse response, the whole impulse response could be rendered useless. This is a problem particularly where the excited structure has strong resonating behavior, such as with vibrating plates. Also an averaging procedure over different frequencies would not be a real improvement because it is still based on unreliable constituents.

Let k indicate the measurement, then we can define an error for the n-th pressure signal $p_n^k(t)$ measured in the far field as follows:

$$e_n^k(t) = p_n^k(t) - \sum_{\tau=0}^{T-1} \mathbf{g}_n^T(\tau)\mathbf{q}^k(t-\tau) \qquad (22)$$

Using the average of the squared value of $e_n^k(t)$ over a sufficiently long period of time and summing the contributions of the different measurements leads to the cost function

$$J_n = \sum_k E\left\{\left[e_n^k(t)\right]^2\right\} \tag{23}$$

Let a correlation matrix $R_{xy}(\tau)$ for arbitrary signal vectors $\mathbf{x}(t)$ and $\mathbf{y}(t)$ be defined by

$$\mathbf{R}_{xy}(\tau)=E\{\mathbf{y}(t+\tau)\mathbf{x}^T(t)\}, \qquad \tau= -T+1, \ldots, T-1, \tag{24}$$

then the cost function can be written as

$$J_n = \sum_k \left[\mathbf{R}_{p_n^k p_n^k}(0) - \sum_{\tau=0}^{T-1} \mathbf{R}_{q^k p_n^k}(\tau) g_n(\tau) - \sum_{\tau=0}^{T-1} \mathbf{g}_q^T(\tau) \mathbf{R}_{q^k p_n^k}^T(\tau) + \sum_{\tau=0}^{T-1}\sum_{\tau'=0}^{T-1} \mathbf{g}_n^T(\tau) \mathbf{R}_{q^k q^k}(\tau'-\tau) \mathbf{g}_n(\tau') \right] \tag{25}$$

The derivative of the cost function with respect to the coefficients $g_n(t)$ can be written as

$$\frac{\partial J_n}{\partial g_n(\tau)} = \sum_k \left[\sum_{\tau'=0}^{T-1} \mathbf{g}_n^T(\tau') \mathbf{R}_{q^k q^k}(\tau-\tau') - \mathbf{R}_{q^k p_n^k}(\tau) \right], \quad \tau = 0, \ldots, T-1 \tag{26}$$

Requiring this derivative to be zero leads to the system of equations

$$\sum_k \sum_{\tau'=0}^{T-1} \mathbf{g}_n^T(\tau') \mathbf{R}_{q^k q^k}(\tau-\tau') = \sum_k \mathbf{R}_{q^k p_n^k}(\tau), \quad \tau = 0, \ldots, T-1 \tag{27}$$

from which $\mathbf{g}_n(t)$ can be solved. The Green's function matrix $\mathbf{G}(t)$ is then assembled from the different $\mathbf{g}_n(t)$ according to Eq. (6). Since the structure in Eq. (27) is block Toeplitz [23], an efficient routine can be used for its solution [24]. A quadratic cost involving the coefficients of g_n was added in order to stabilize the solution. The cost function actually minimized was:

$$J_n = \sum_k E\left\{\left[e_n^k(t)\right]^2\right\} + \beta \sum_{\tau=0}^{T-1} \mathbf{g}_n^T(\tau) \mathbf{g}_n(\tau) \tag{28}$$

with ß a weighting coefficient for the Green's function coefficients. In addition, a frequency dependent weighting can be applied that corresponds to the frequency range for which the radiation modes have to be determined. The different excitation patterns k could also be applied simultaneously, leading to an improved signal to noise ratio. In that case, instead of using a block Toeplitz inversion scheme, it would be possible to use an adaptive algorithm, such as a least-mean-square algorithm, to search for the coefficients of the Green's function. If the Green's function contains strongly resonating behavior, such as in an enclosed space, then it may be advantageous to combine information regarding the poles of the system, such as with a state-space description [25].

2.2 Reciprocal method

In this subsection it is shown that reciprocal techniques can be used favorably for the actual measurement of radiation modes. As discussed in the previous subsection, the Green's function is needed that expresses the response in the far field in terms of elementary sources on the structure. In case of radiation modes for velocity sensing which lead to the pressure in the far field of a halfspace, we need the transfer function g_{mn} from (volume) velocity at the structure to pressure in the far field. A reciprocity relationship [26] exists between the pressure and volume velocity at two different positions $\mathbf{x}_n$ and $\mathbf{x}_m$:

$$\frac{p^A(\mathbf{x}_n)}{q^A(\mathbf{x}_m)} = \frac{p^B(\mathbf{x}_m)}{q^B(\mathbf{x}_n)} \tag{29}$$

where A denotes the situation in which the source is at position $\mathbf{x}_m$ and the receiver is at position $\mathbf{x}_n$, and B denotes the situation in which the source is at position $\mathbf{x}_n$ and the receiver is at position $\mathbf{x}_m$. In the present context A is the direct method and B is the reciprocal method. If the original notation is used

this becomes: $p^A_m/q^A_m = p^B_m/q^B_n$. This means that placing a source with known volume velocity in the far field and measuring the *pressure* on the structure leads to Green's functions that can be used to obtain the radiation modes for *velocity* sensing on the structure. The advantage of the reciprocal technique is that much larger sources can be used for measuring the transfer functions and that the responses can be obtained almost directly at the radiating surface. It is noted that the reciprocal technique can be used equally well for measuring radiation modes in enclosed spaces, which in this case are the velocity patterns that contribute to the potential energy in the enclosure.

2.3 Combined inverse and reciprocity method

In Subsection 2.1 a method was given to obtain radiation modes after excitation of the structure with different excitation patterns and the acquisition of the resulting structural sensor signals and far field pressure signals. The available actuators can often be used to generate the excitation patterns for plate vibration in order to extract the radiation modes. In such cases two types of transfer functions are required: the transfer from actuator drive signal to structural sensor and the transfer from actuator drive signal to far field sensor. Measurement of the first type of transfer function usually gives no problems. However, measurement of the second type of transfer functions can be troublesome due to large background noise, especially if the actuators are relatively small. In such cases it can be better to use a reciprocal technique for measuring the transfer from actuator drive signal to the far field signal, which is obtained by using the actuator as sensor.

Assume that a set of reciprocal actuators is used which can be operated both as actuator and as sensor, each used as actuator by driving with a certain current, and being used as a sensor by measuring the voltage, then combining Eq. (29) with the results of the section on reciprocity in transducers in Pierce [16], the following relationship can be derived for the k-th actuator:

$$\frac{p^A(\mathbf{x})}{i_k^A} = -\frac{e_k^B}{q^B(\mathbf{x})} \tag{30}$$

where e is the voltage on the actuator, q is the volume velocity of an acoustic source, p is the pressure in the field, and i is the current going through the actuator. Further, A denotes the situation in which actuator k is driven by a current source i and in which the resulting pressure p at far field position $\mathbf{x}$ is measured, and B denotes the situation in which a source of volume velocity q at far field position $\mathbf{x}$ is used and in which the resulting voltage e at actuator k is measured. It is noted that coordinate $\mathbf{x}$ corresponds to far field position n, as used previously. That Eq. (30) is valid in a large frequency range can be seen in Figure 1. Larger differences can be found at low frequencies but this is the region where the direct method suffers from noise. The curves from the reciprocal method behave as expected, also at low frequencies.

3 Actuator modes

The broadband radiation mode formulation can also be used for the design of signal processing schemes that drive an array of actuators. As will become apparent from the description below, a control scheme as shown in figure 11b can advantageously be used in a broadband scheme according to the invention. Figure 11b shows an object 1a, 1b e.g., a plate (that may have an arbitrary shape and may be located in an enclosure), that is made to vibrate by means of a plurality of actuators 3a. The primary sound field is due to a source (2) which produces primary vibrations of the structure. Although the primary source (2) as indicated in Figure 11b is an acoustic source, the actual primary source can also be a mechanical primary source which directly excites the structure. The actuators 3a may be piezo-electric transducers or shakers driven by a driving signal $\mathbf{u}$. Object 1 also contains a plurality of sensors 3b. In a preferred embodiment the sensors 3b consist of piezoelectric transducers and may be combined with the actuators 3a into the same physical transducers.

Each of the sensors 3b produce an output signal corresponding with quantity **q** (e.g. velocity or pressure or strain). The output signals **q** are received by a controller 5.

The controller 5 comprises means for multiplying the output signals **q** by the radiation modes **E**. The resulting signals are summed to render error signals **v**, in accordance with Eq. (18). Block 11 denotes that the controller 5 is arranged with means to (optionally) perform a frequency dependent weighting operation **K** on error signals **v** to provide resulting error signals **e** (equation (20)). The resulting error signals e are used by the controller 5 to control adaptive parameters of an adaptive controller 13. Adaptive controller 13 produces output signals applied to a filter 15 with fixed filter coefficients **W'**. Filter 15 produces actuator drive signals **u**. These actuator drive signals **u** are optionally amplified.

The controller 5 has been shown in a very schematic way to clearly demonstrate the different signals of the calculations presented here. The blocks shown in controller 5 need not be physically present. There may be just one processor performing all the necessary calculations and simulating the block scheme of figure 11b . Alternatively, the controller may be designed with different parallel operating processors or with processors in a master-slave configuration, as is known to persons skilled in the art. Basically, there is no restriction as to how the controller is designed as long as it is capable of performing the essential features of the annexed claims. Even analoque and/or digital circuits can be used, as the case may be.

As compared to the radiation mode schemes for sensors, modal schemes for actuators have additional requirements. Like the sensor scheme, the actuator scheme is required to consist of a set of nearly independent driving patterns, the so-called actuator modes, that have good sensitivity for sound radiation in the frequency range where sound power reductions have to be obtained. This frequency range is usually the low frequency range. In addition, the actuator configuration is preferably designed in such a way that,

in the frequency range where the nearfield sensor configuration fails to predict the farfield sound field, usually in the high frequency range, the actuator modes have a small sensitivity for sound radiation. In other words, the configuration is preferably designed in such a way that it has a minimum of 'spillover'. In the following a method is given to statisfy these requirements using a given physical actuator configuration. As opposed to approaches in which the positions of the actuators are optimized [27], the present formulation optimizes a signal processing scheme for a given actuator array. The advantage is that the system can be calibrated in-situ with measured transfer functions using an identical actuator array which can be used for different situations.

3.1 Cost function for actuator modes

Numerical experiments were performed to investigate the possibility of using simple coefficients for the actuator configuration, similar to the techniques used for the sensor configuration. One of the techniques that was tried was to determine arrays of weighting coefficients based on the eigenvalues of the squared transfer function between actuator drive signals and pressure signals in the far field, under the condition that they were orthogonal to a selected set of constraint vectors [28].
These methods were found to be able to reduce spill-over effects. Instead of using simple, frequency independent, weighting coefficients, the following descriptions assume frequency dependent filters. However, simple weighting coefficients might also be used, possibly at the cost of a reduction of the performance.

One approach is a technique to minimize the modal contributions due to the secondary path which are not taken into account by error sensors. The secondary path is the path followed by the signals produced by the actuators to the error sensors. As compared to the method of Morgan [15], the present description gives an extension to broadband signals and an

optimization for acoustic radiation and not simply mechanical vibration. Still a further extension is that a systematic method is presented to reduce spillover at high frequencies by defining two different sets of vibration patterns, one set of which is used for good sound power reductions at low frequencies, while the other set is used for the reduction of spillover.

For the moment it will be assumed that the configuration is feedforward. Let $\mathbf{u}(t) = [u_1(t)u_2(t) \ldots u_K(t)]^T$ be the vector of actuator control signals, which is obtained by filtering the reference signal vector $\mathbf{x}(t) = [x_1(t)x_2(t) \ldots x_L(t)]^T$ with a matrix $\mathbf{W}(t)$ of finite impulse response filters:

$$\mathbf{u}(t) = \sum_{\tau=0}^{T-1} \mathbf{W}(\tau)\mathbf{x}(t-\tau) \tag{31}$$

It is observed that matrix $\mathbf{W}(t)$ is represented in figure 11b by both the adaptive controller 13 ($\mathbf{W}''$) and the filter $\mathbf{W}'$ with fixed coefficients $\mathbf{W}'_{km}$.

Further, let $\mathbf{q}_s(t)$ be the vector of secondary signals at the sensors (i.e. the output signals of sensors 3b due to input signals $\mathbf{u}$), and let $\mathbf{H}(t)$ be the matrix of transfer functions of the secondary path from actuator signal vector to sensor signal vector, as in

$$\mathbf{q}_s(t) = \sum_{\tau=0}^{T-1} \mathbf{H}(\tau)u(t-\tau) \tag{32}$$

The radiation mode sensor signal vector for the observed radiation modes in $\mathbf{E}$ due to the secondary sources (i.e. the actuators 3a) is

$$\mathbf{u}_s(t) = \mathbf{E}^T\mathbf{q}_s(t) \tag{33}$$

The corresponding signal vector after frequency dependent weighting is given by

$$\mathbf{s}(t) = \sum_{\tau=0}^{T-1} \mathbf{K}(\tau)\mathbf{v}_s(t-\tau) \tag{34}$$

The total error signal vector is simply the sum of a primary signal vector (i.e. a vector related to a primary disturbance source) and the secondary signal vector given by

$$\mathbf{e}(t) = \mathbf{d}(t) + \mathbf{s}(t) \tag{35}$$

with $\mathbf{d}(t)$ a primary disturbance signal vector of weighted radiation modal sensors. Thus, if a primary sensor signal vector (i.e. output signal of sensors 3b due to the primary source) is given by $\mathbf{q}_d(t)$, then $\mathbf{d}(t)$ can be obtained from the subsequent operations

$$\mathbf{u}_d(t) = \mathbf{E}^T\mathbf{q}_d(t) \tag{36}$$

and

$$\mathbf{d}(t) = \sum_{\tau=0}^{T-1}\mathbf{K}(\tau)\mathbf{v}_d(t-\tau) \tag{37}$$

We also define error signals for unobserved modes. The radiation modal sensor signal vector due to the secondary sources (i.e. the actuators 3a) for a selected set of unobserved radiation modes $\mathbf{E}'$, termed constraint modes, is

$$\mathbf{u}_{s'}(t) = \mathbf{E}'^T\mathbf{q}_s(t) \tag{38}$$

The corresponding signal vector after frequency dependent weighting is given by

$$\mathbf{s}'(t) = \sum_{\tau=0}^{T-1}\mathbf{K}(\tau)\mathbf{v}_{s'}(t-\tau) \tag{39}$$

Finally, the error criterion is defined as

$$J = E\{\mathbf{e}^T(t)\mathbf{e}(t)\} + \beta_1 tr.\left\{\sum_{\tau=0}^{T-1}\mathbf{W}^T(\tau)\mathbf{W}(\tau)\right\} + \beta_2 E\{\mathbf{u}^T(t)\mathbf{u}(t)\} + \beta_3 E\{\mathbf{s}'^T(t)\mathbf{s}'(t)\} \tag{40}$$

where tr. denotes a trace operator, which is known as such. The first part of the cost function minimizes the error signal on the observed modes, the second part minimizes the filter coefficients, the third part minimizes the control effort, and the fourth part minimizes the secondary path signals that are not observed by the error sensors. The minimization of this equation can be obtained by using efficient methods for block-Toeplitz matrices [24]. Usually, only one of the parameters β_1, β_2 or β_3 is used for the computation of **W**.

Figure 10 shows a possible configuration for a feedback controller. With this particular configuration the contribution of the secondary path on the reference signal **x** is subtracted in the controller, which leads to an input signal on the controller **W** which only consists of the primary signal v_d. This is accomplished by subtracting from the measured signal **v** the secondary path signal v_s. Under these conditions, the input signal to the controller is unrelated to the secondary signals and consists only of the primary signal v_d. Then, the configuration can be regarded as feedforward and the design techniques of feedforward control systems apply.

If the optimum filter is computed in such a way that the optimum filter **W** is a causal inverse of the transfer functions between actuators and sensors, thereby taking into account constraints such as described above, then this particular $\mathbf{W} = \mathbf{W}'$ can be used as a preconditioner [29] in an adaptive algorithm. The preconditioner can be computed off-line. A possible practical implementation of such a scheme with a preconditioner **W'** and an adaptive controller **W"** is shown in Figure 11b. Alternatively, the filter **W** can be obtained in an iterative way where the various error signals and constraints are taken into account in the iteration scheme.

In addition to a slower convergence [29], the latter technique has the disadvantage that the number of computations is larger than for the preconditioned scheme.

3.2 Selection of constraint modes

As described in Section 1, a method to obtain **E** is by low-pass filtering of the Green's functions if reductions at low frequencies have to be obtained. Usually, the constraint modes **E'** can not be obtained from the same technique. This is due to the fact that the modes in **E'** should be the modes that are efficient radiators at high frequencies only. Therefore, a low pass filtering operation of the Greens' functions would eliminate these components, which is undesirable. Also a high-pass filtering of the Green's function is inadequate because the resulting radiation modes are not only efficient radiators at high frequencies, but also possibly efficient radiators at low frequencies. In the following a method is given to compute the modes **E'** that are the most efficient radiators in a broadband sense under the constraint that they are orthogonal to the modes **E** which have previously been found as the most efficient radiators at low frequencies. This implies that the modes **E'** are efficient radiators at high frequencies and inefficient radiators at low frequencies. Hence, the modes **E'** can be used as constraint vectors in order to optimize the actuator configuration.

As described above, it would be desirable to have an actuator array that has a good coupling with respect to a certain quantity and simultaneously a minimum amount of coupling with respect to another quantity. In this section it is shown how these two goals can be accomplished. In particular, the modes of $\mathbf{P}_{GG}(0)$ are computed using the constraint that they are orthogonal to r vectors in an M x r dimensional matrix **E**. If the desired modes are the columns of the M-row matrix **E'**, then the constraint can be expressed as

$$\mathbf{E}^T\mathbf{E}' = \mathbf{0}. \tag{41}$$

Following Golub and van Loan [28] and assuming an M x M dimensional matrix **Q**, an M x r dimensional matrix **S**, and an r x r dimensional matrix **Z**, the singular value decomposition of **E** is computed as

$$\mathbf{E} = \mathbf{Q}\mathbf{S}\mathbf{Z}^T \tag{42}$$

An M x M dimensional matrix $\mathbf{B}$ is formed from

$$\mathbf{B} = \mathbf{Q}^T\mathbf{P}_{GG}(0)\mathbf{Q} \tag{43}$$

where the Green's functions $\mathbf{G}$ leading to $\mathbf{P}_{GG}(0)$ are possibly high-pass filtered. Assuming an $(M - r)$ x $(M - r)$ dimensional matrix $\mathbf{B}_{22}$, the matrix $\mathbf{B}$ is partitioned as follows:

$$\mathbf{B} = \begin{bmatrix} \mathbf{B}_{11} & \mathbf{B}_{12} \\ \mathbf{B}_{21} & \mathbf{B}_{22} \end{bmatrix} \tag{44}$$

Eigenvectors $\mathbf{V}_{B22}$ are found from the decomposition

$$\mathbf{B}_{22} = \mathbf{V}_{B22}\mathbf{\Lambda}_{B22}\mathbf{V}^T_{B22} \tag{45}$$

Upon construction of the M x $(M - r)$ dimensional matrix

$$\mathbf{Y} = \begin{bmatrix} 0 \\ \mathbf{V}_{B22} \end{bmatrix} \tag{46}$$

where the $\mathbf{0}$ is a zero matrix of dimensions r x $(M - r)$, the $M - r$ constrained eigenvectors in the M x $(M - r)$ dimensional matrix $\mathbf{E}'$ follow from

$$\mathbf{E}' = \mathbf{QY} \tag{47}$$

The vectors in the columns of $\mathbf{E}'$ are the most significant modes in $\mathbf{P}_{GG}(0)$ under the condition that they are orthogonal to the column vectors in $\mathbf{E}$. Simplifications of the computational procedure are possible if the vectors in $\mathbf{E}$ are orthonormal. As with the radiation modes E as described in Section 2, the constraint modes $\mathbf{E}'$ can be obtained from an in-situ calibration procedure, since the constraint modes $\mathbf{E}'$ are also based on the Green's function matrix $\mathbf{G}$ and filtered versions thereof.

4 Results

4.1 Radiation mode shapes for velocity sensing

As a simple example, radiation mode shapes were computed with Eq. (17) based on the monopole space-time domain Green's function for a baffled radiator (see, for instance, Eq. (5-2.1) in [16])

$$g_{mn}(t) = S_m \frac{\rho}{2\pi} \frac{\partial}{\partial t} \frac{\delta(t - \tau_{mn}/c}{T_{mn}} \tag{48}$$

where t denotes continuous time, ρ is the density of air, S_m is the area of a so-called elemental radiator [4], δ is a temporal Dirac impulse function, c = 343 m/s is the speed of sound, and $r_{mn} = \| \mathbf{x}_m - \mathbf{x}_n \|$ is the distance between source coordinate $\mathbf{x}_m$ and receiver coordinate $\mathbf{x}_n$. Discrete-time representations $g_{mn}(t)$ were obtained by linear interpolation, using samples of Eq. (48). Source points were assumed to be distributed over a rectangular area of 60 cm x 75 cm, using 5 x 6 sources. The pressure was recorded at 12 positions on a hemisphere with a radius of 5 m according to the AS1217.6-1985 standard, as described in [30]. The Greens' function was low pass filtered at a frequency f = 288 Hz, which corresponds to $ka = 2$, with $k = \omega/c$ the wavenumber, $\omega = 2\pi f$ the angular frequency, and a = 0.3785 m, being an effective radius of the total radiator. The low-pass filter and the differentiator were implemented with 21-tap and 11-tap FIR filters, respectively.

The first four resulting radiation modes are shown in Figures 2a, 2b, 2c, 2d, and the thirty normalized eigenvalues in Figure 3. In addition, radiation modes and normalized eigenvalues were computed with a frequency domain technique using $\mathbf{R}(\omega)$ at $ka = 2$ [4] (Figures 4a-4d and 5), and with the same frequency domain technique using an averaging of $\mathbf{R}(\omega)$ over $0 \leq ka \leq 2$ (Figure 6a-6d and 7). The time domain result and the averaged frequency domain result are nearly equal, as expected. Also the eigenvalues are nearly equal. The shapes and eigenvalues of the frequency domain modes at $ka = 2$ differ somewhat more, also as expected.

4.2 Estimation of radiation modes from measurable transfer functions

The method of Section 2 was used to estimate the time domain Green's function $\mathbf{G}(t)$ and the resulting broadband radiation modes $\mathbf{E}$. The discrete-time Green's function corresponding to Eq. (48) was estimated by exciting a plate with 30 piezoelectric patch actuators [12]. For each actuator, the resulting velocities at 30 positions on the plate were recorded as well as the pressure at 12 positions in the far field of the plate. For the velocity and pressure sensors, the same positions were used as in Subsection 4.1.

The value of ß was set to such a value that the relative mean-squared contribution of ß $\sum_{\tau=0}^{T-1}\mathbf{g}_n^T(\tau)\mathbf{g}_n(\tau)$ to the diagonal of the matrix resulting from $\sum_k \mathrm{E}\{[\, e_n^k(t)]^2\}$ was equal to 10^{-4}. In the simulations, a simply supported aluminium sandwich plate of 6 mm thickness was used. The width and height were 60 cm and 75 cm, respectively. The plate density was taken to be $\rho_p = 870$ kg m^{-3}, the Young's modulus as $E = 3.6 \times 10^{10}$ Pa, and the hysteretic damping as $\eta = 0.02$, except for the (1,1) plate mode for which a larger damping $\eta = 0.1$ was used. The number of plate modes taken into account was 8 x 8. The Greens function coefficients were collected in a 30 x 12 matrix of FIR filters having 32 samples each, using a sampling frequency of 1 kHz.

The resulting first four radiation modes are shown in Figures 8a-8d and the corresponding eigenvalues in Figure 9. It can be seen that the shapes of the first three modes (Figures 8a-8c) are similar to the corresponding shapes in Figure 2. The shape of the fourth mode in Figure 8d is different from the one in Figure 2d. This can be explained by looking at the eigenvalues in Figure 9. It can be seen that the fourth-order eigenvalue and other high-order eigenvalues have a much lower value than the first three eigenvalues, and therefore are relatively unimportant. Errors due to the reconstruction process

can lead to changes from the theoretical results, especially for the small eigenvalues. However, small reconstruction errors should not have a significant effect on large eigenvalues, as can be seen in the results. This was supported by other numerical experiments.

4.3 Design of a modal actuator with application to feedback ASAC

Numerical results are presented for the general cost function of Eq. (40). A simulation example is given of the design of an actuator array for use in active structural acoustic control. Both the sensor array and the actuator array consist of piezoelectric patch transducers and are shown in Figure 12.

For the error signal **e**, 3 radiation modes were used. The modes **E** were obtained by low-pass filtering the Greens' function at 288 Hz, computing the eigenvectors of the transfer correlation matrix, and using the three strongest modes. The constraint modes **E'** were obtained by an eigenvector computation based on the unfiltered Green's function under the constraint that they had to be orthogonal to the three modes in **E**, as described in Subsection 3.2. The parameters of the plate were the same as in the previous example. An analytical method for the computation of weighting coefficients for the piezoelectric sensor array was used, as described previously [31]. Together with the radiation modes **E** and **E'** these weighting coefficients could be used to derive radiation modal error signals and constraint signals, respectively, for a piezoelelectric sensor array. In [31], no frequency dependent weighting was used. In order to improve the performance, for the present example a frequency dependent weighting was used, which was based on the diagonal of Eq. (21) for both **E** and **E'**.

The control configuration was based on Internal Model Control [32], where the contribution $\mathbf{v}_s$ of the secondary path on the detection signal vector was subtracted from the measured signal vector **v** in the controller (Figure 10). In this way the controller coefficients **W** and the resulting performance of the system could be computed by using the techniques for feedforward control. The

configuration was a feedback system where the reference signals $\mathbf{x}(t)$ were equal to the unfiltered radiation modal error signals $\mathbf{v}_d(t)$, and where the signals $\mathbf{d}(t)$ and $\mathbf{s}(t)$ were obtained by a frequency dependent filtering of the radiation modal error signals, by using the diagonal of matrix $\mathbf{K}(t)$. The frequency dependency was implemented by a least-squares fit of the frequency dependent efficiency of the radiation modes, using the Matlab function firls. The order of the filters was chosen to be 10.

The incident field was an impulsive plane wave incident on the plate at directions $\theta = \pi/3$ en $\varphi = \pi/3$ to the plate normal. The sampling frequency was 1 kHz and the length of each of the filters of $\mathbf{W}$ was 256, resulting in a total number 30 of coefficients of 256 x 3 x 9 = 6912. A controller delay of 1 sample was assumed. The radiated sound power was evaluated by computing the plate velocity before control and after control at 10 x 10 positions.

The influence on the performance of each of the individual parameters β_1, β_2 and β_3 was investigated. For each of these parameters, a value could be found for which the reduction of the broadband radiated sound power was maximum. The results which are shown are at these maximum values of reduction. The results are given in Figure 13. The broadband reductions for coefficient weighting with β_1, effort weighting with β_2, and radiation modal constraint weighting with β_3 (cf. Eq. (40)) are 8.0 dB, 6.7 dB, and 9.9 dB, respectively. Especially at high frequencies the performance with modal constraint weighting is better than with the other two methods. For configurations having less symmetry than the present configuration the results substantially degrade for weighting with β_1 or β_2, while being relatively close to the above result for weighting with β_3. Additionally, it was found that the performance depended less critically on the actual value of β_3 than on β_1 or β_2. It can also be seen that the result for modal constraint weighting is the only result which does not lead to increases at any frequency. According to an approximate formula [9], the maximum frequency for which significant

reductions can be obtained using 3 radiation modes for a plate of 60 cm x 75 cm is approximately 300 Hz, which agrees with the results of Figure 13.

Instead of using a simultaneous minimization of the radiation modal error signals, the cost function J was also minimized for each of the radiation modal error signals independently. Considering the optimal filters for a particular radiation modal error signal, the constraint modes were augmented with the remaining radiation modes, which are two modes in this case. The results were similar to the previous results with slightly smaller reductions, being 7.6 dB, 6.7 dB and 8.5 dB, for weighting with β_1, β_2 and β_3, respectively. The advantage is that the systems obtained in this way are more robust than those obtained from the simultaneous minimization of the radiation modal error signals. The quantification of robustness was based on a method described by Elliott [33]. The maximum singular value of 30 the open-loop gain at any frequency was 700 for the simultaneous optimization and approximately 20 for the independent minimization. It is noted that the latter configuration is a true modal actuator, and therefore the adaptive filter could be chosen to be diagonal. In other words, each radiation modal error signal could be controlled independently by the corresponding radiation modal actuator.

The simultaneous minimization procedure leads to a fully coupled controller, i.e., secondary signals are generated on all radiation modal error sensors for each radiation modal reference signal. Apparently, the additional freedom allowed in the simultaneous minimization procedure is used by the algorithm to create a fully coupled controller in order to be able to fulfill to a further extent the concurring requirements imposed on radiation modal error signals and contribution of the secondary path on the constraint modes.

In the present examples the number of actuators is larger than the number of error signals. Also for the case where the number of actuators was less than or equal to the number of error signals the performance of the modal weighting scheme was found to give the largest reduction of broadband

radiated sound power. However, for that case the differences were smaller, especially between effort weighting and modal constraint weighting.

In the present description finite impulse response (FIR) filters were assumed for the Green's function **G**, for the secondary path **H**, for the frequency dependent weighting matrix **K**, and for the controllers **W**, **W'**, **W''**. It is noted that the methods as described in the present invention are not limited to FIR filters but can be based on other models, such as Infinite Impulse Response (IIR) filters, state-space implementations, or still other implementations. It is also noted that other control strategies are possible than Internal Model Control, which was used in the examples.

It is interesting to compare the present technique with the technique described by Elliott et al. [32]. In the latter paper, a method is described to reduce the primary field at microphones in the far field by feedback of the structural sensor signals. A property of this method is that a control filter is required between each structural sensor and each actuator. For the present configuration this would lead to a nine times increase of the dimensionality of the adaptive controller, viz. from 3 x 3 to 9 x 9. The technique of Elliott et al. gives the possibility of limiting the control effort at high frequencies but this would not lead to a more efficient implementation. A more efficient implementation of the sensor, valid for $ka < 1$, is obtained by combining the structural sensor signals into a single radiation modal sensor signal, such as described by Sors [34]. The techniques of the present invention give extensions for: higher order radiation modes (i.e. reductions also for $ka \geq 1$), a method for the design of modal actuators, the reduction of controller dimensionality, a method to limit undesired sound power increases at high frequencies, and a suggested technique to obtain radiation modes in situ.

5 Conclusions

Above, methods have been presented to obtain the most efficiently radiating vibration patterns of an object, termed radiation modes, by using a

broadband formulation. It has been shown that a radiation mode formulation based on a description in the time domain can be used to arrive at efficient schemes for reduction of sound radiated from objects. The resulting modes were called broadband radiation modes because they are the optimum modes in a broadband sense. This is in constrast with existing techniques which are based on radiation modes determined at a single frequency but which are often used to control broadband radiation. Frequency dependent weighting schemes for the broadband radiation modes have been presented.

For a baffled plate, for which analytical descriptions of relevant Green's functions are available, it has been shown that the radiation modes for velocity sensing obtained from a low-pass filtered Green's function are equivalent to conventional radiation modes obtained from an averaging in the frequency domain.

A method was given to determine the radiation modes in-situ, in which case the relevant Green's function is usually unknown.

Finally, the broadband radiation modes were used to obtain driving schemes for a configuration consisting of arrays of piezoelectric sensors and piezoelectric actuators. Three methods for the derivation of the driving schemes were compared.

It has been shown that an optimum filter based on constraints on a special set of vibration patterns, of which the outputs were weighted with frequency dependent filters, gave better results than that obtained with coefficient weighting and control effort weighting. These constraint patterns were computed in such a way that they were inefficient radiators at low frequencies and efficient radiators at high frequencies. In addition the new weighting scheme was found to be less sensitive to changes in the configuration. Also the choice of the weighting parameter was less critical. In this way efficient modal sensors and modal actuators can be designed having a good tradeoff between large sound power reductions in the controlled

frequency range and a minimum of increased sound power in the uncontrolled frequency range.

Appendix A Completeness of averaged radiation matrices

In this appendix a proof is given of the completeness of the eigenvectors of an averaged radiation matrix. In particular, it is shown that the subspace spanned by the significant eigenvectors of an averaged radiation matrix $\overline{\mathbf{R}}$ equals the subspace spanned by the significant eigenvectors at the highest frequency over which the averaging is performed. Positive angular frequencies ω_k are assumed which are increasing with index k, i.e. $0<\omega_k<\omega_{k+1}$. The radiation matrix $\hat{\mathbf{R}}(\omega)$ is defined such that $\hat{\Pi}(\omega) = \hat{\mathbf{q}}^H(\omega)\hat{\mathbf{R}}(\omega)\hat{\mathbf{q}}(\omega)$ is the radiated power. Further, the radiation matrix $\hat{\mathrm{R}}(\omega)$ at $\omega = \omega_k$ is denoted by $\mathbf{R}_k$.

Assuming an eigenvector decomposition $\mathbf{R}_k = \mathbf{E}_k\mathbf{D}_k\mathbf{E}_k^T$ with $\mathbf{E}_k = \{E_1^k, E_2^k, \ldots, E_m^k\}$ and $\mathbf{D}_k = \mathrm{diag}\{d_1^k, d_2^k, \ldots d_m^k\}$ a diagonal matrix with the eigenvalues in decreasing order, the range of $\mathbf{R}_k$ is defined as the span of its significant eigenvectors $\{E_1^k, E_2^k, \ldots, E_j^k\}$:

$$\text{range } \mathbf{R}_k = \text{span}\{E_1^k, E_2^k, \ldots, E_j^k,\ d_p^k > \varepsilon\ \forall p \in \{1, \ldots, l\}) \quad \text{(A1)}$$

where ε is a fixed positive threshold. Using $\overline{\mathbf{R}} = \sum_{k=1}^{K}\mathbf{R}_k$, the range of the averaged radiation matrix is given by [28]

$$\text{range } \overline{\mathbf{R}} = \text{range}\sum_{k=1}^{K}\mathbf{R}_k = \text{range } \mathbf{R}_1 + \text{range } \mathbf{R}_2 + \ldots + \text{range } \mathbf{R}_K \quad \text{(A2)}$$

In view of the conjecture of Borgiotti and Jones [5]:

$$\text{range } \mathbf{R}_k \subset \text{range } \mathbf{R}_{k+1} \text{ (nesting property)}, \quad \text{(A3)}$$

it is easily shown that Eq. (A2) leads to

$$\text{range } \overline{\mathbf{R}} = \text{range } \mathbf{R}_K, \quad \text{(A4)}$$

which is the desired result, because range R_K provides a complete set of basis functions for the reduction of sound radiation for all frequencies below ω_K. The above procedure also applies to an averaging procedure based on an integral over ω instead of a summation, which, in view of the integral of Eq. (11) and the identification $\hat{\mathbf{P}}(\omega) = \hat{\mathbf{R}}(\omega)$, demonstrates the completeness of the eigenvectors $\mathbf{E}$ obtained from Eq. (17). For many geometries the eigenvectors of $\overline{\mathbf{R}}$ that are efficient radiators at low frequencies are efficient radiators also at high frequencies. Therefore these eigenvectors are weighted more heavily, i.e. have larger eigenvalues, than the eigenvectors of $\overline{\mathbf{R}}$ that are efficient radiators mainly at high frequencies.

References

[1] G.V. Borgiotti. The power radiated by a vibrating body in an acoustic fluid and its determination from boundary measurements. *J Acoust Soc Am*, 88:1884–1893, 1990.

[2] D.M. Photiadis. The relationship of singular value decomposition to wave-vector filtering in sound radiation problems. *J Acoust Soc Am*, 88:1152–1159, 1990.

[3] A. Sarkissian. Acoustic radiation from finite structures. *J Acoust Soc Am*, 90:574–578, 1991.

[4] S.J. Elliott and M.E. Johnson. Radiation modes and the active control of sound power. *J Acoust Soc Am*, 94:2194–2204, 1993.

[5] G.V. Borgiotti and K.E. Jones. Frequency independence property of radiation spatial filters. *J Acoust Soc Am*, 96:3516–3524, 1994.

[6] K.A. Burgemeister. Novel methods of transduction for active control of harmonic sound radiated from vibrating surfaces. Ph.D. thesis, University of Adelaide, 1996.

[7] B.S. Cazzolato and C.H. Hansen. Structural radiation mode sensing for active control of sound radiation into enclosed spaces. *J Acoust Soc Am*, 106:3732–3735, 1999.

[8] G.P. Gibbs, R.L. Clark, D.E. Cox, and J.S. Vipperman. Radiation modal expansion: Application to active structural acoustic control. *J Acoust Soc Am*, 107:332–339, 2000.

[9] A.P. Berkhoff. Sensor scheme design for active structural acoustic control. *J Acoust Soc Am*, 108:1037–1045, 2000.

[10] B.S. Cazzolato and C.H. Hansen. Active control of sound transmission using structural error sensing. *J Acoust Soc Am*, 104:2878–2889, 1998.

[11] A. Preumont, A. Francois, and S. Dubru. Piezoelectric array sensing for real-time, broad-band sound radiation measurement. *Journal of Vibration and Acoustics*, 121:446–452, 1999.

[12] C.R. Fuller, S.J. Elliott, and P.A. Nelson. *Active control of vibration.* Academic Press, London, 1996.

[13] C.-K. Lee and F.C. Moon. Modal sensors/actuators. *Transactions of the ASME*, 57:434–441, 1990.

[14] W. Gawronski. Modal actuators and sensors. *J Sound Vib*, 229:1013–1022, 2000.

[15] D.R. Morgan. An adaptive modal-based active control system. *J Acoust Soc Am*, 89:248–256, 1991.

[16] A.D. Pierce. *Acoustics - An introduction to its physical principles and applications.* Acoustical Society of America, Woodbury, New York, 2 edition, 1989.

[17] R.A. Roberts and C.T. Mullis. *Digital signal processing.* Addison Wesley, Reading, 1987.

[18] L. Ljung. *System Identification - Theory for the User.* Prentice-Hall, Englewood Cliffs, 1987.

[19] S. Skogestad and I. Postlethwaite. *Multivariable feedback control.* John Wiley and Sons, Chichester, 1996.

[20] S.L. Marple Jr. *Digital spectral analysis with applications.* Prentice-Hall, Englewood Cliffs, 1987.

[21] D.C. Youla. On the factorization of rational matrices. *IRE Trans Inform Theory*, IT-7:172–189, 1961.

[22] W.T. Baumann, W.R. Saunders, and H.H. Robertshaw. Active suppression of acoustic radiation from impulsively excited structures. *J Acoust Soc Am*, 90:3202–3208, 1991.

[23] J. Chun and T. Kailath. Generalized displacement structure for block-toeplitz, toeplitz-block, and toeplitz derived matrices. In G.H. Golub and P.v. Dooren, editors, *Numerical linear algebra, digital signal processing and parallel algorithms*, pages 215–236. Springer Verlag, 1991.

[24] E.A. Robinson. *Multichannel time series analysis with digital computer programs.* Holden-Day, San Fransisco, revised edition, 1978.

[25] A. Gelb, J.F. Kasper, R.A. Nash, C.F. Price, and A.A. Sutherland. *Applied optimal estimation*. MIT Press, Cambridge, 11 edition, 1989.

[26] J.T. Fokkema and P.M. van den Berg. *Seismic applications of acoustic reciprocity*. Elsevier, Amsterdam, 1993.

[27] R.L. Clark. Adaptive structures: compensators by design. In S. Douglas, editor, *Proc. Active 99*, pages 63–72. Institute of Noise Control Engineering of the USA, 1999.

[28] G.H. Golub and C.F. Van Loan. *Matrix Computations*. John Hopkins, Baltimore, 2 edition, 1989.

[29] S.J. Elliott. Optimal controllers and adaptive controllers for multichannel feedforward control of stochastic disturbances. *IEEE Transactions on Signal Processing*, 48:1053–1060, 2000.

[30] D.A. Bies and C.H. Hansen. *Engineering Noise Control*. Unwin Hyman, London, 1988.

[31] A.P. Berkhoff. Piezoelectric sensor configuration for active structural acoustic control. *J Sound Vib*, accepted for publication, 2001.

[32] S.J. Elliott, T.J. Sutton, B. Rafaely, and M.E. Johnson. Design of feedback controllers using a feedforward approach. In S.D. Sommerfeldt and H. Hamada, editors, *Proc. ACTIVE 95*, pages 863–874, 1995.

[33] S.J. Elliott. *Signal processing for active control*. Academic Press, 2001.

[34] T.C. Sors. Active structural acoustic control of sound transmission through a plate. Ph.D. thesis, University of Southampton, 2000.

Claims

1. Anti noise system for suppressing primary signals in a space due to a primary source (2), comprising:
   - one or more secondary sources (3a) to produce secondary signals to suppress said primary signals in said space;
   - one or more sensors (3b) to produce sensor output signals (**q**) in relation to said one or more secondary sources (3a);
   - a controller arranged to:
     – receive said sensor output signals (**q**);
     – calculate error signals (**v**) by weighing said sensor output signals (**q**) with radiation mode shapes (**E**) determined for at least one predetermined frequency;
     – use said error signals (**v**) to control an adaptive filter to produce drive signals (**u**) for said secondary sources (3a);

   wherein said controller (5) is also arranged to
     – calculate said error signals (**v**) by weighing said sensor output signals (**q**) with radiation mode shapes (**E**) determined for a plurality of frequencies in a predetermined frequency band.
2. Anti noise system according to claim 1, wherein said system is arranged to determine said radiation mode shapes (**E**) as an average over said plurality of frequencies.
3. Anti noise system according to any of the preceding claims, wherein said system is arranged to calculate said error signals (**v**) by weighing said sensor output signals (**q**) with only those radiation mode shapes (**E**) that are above a predetermined threshold.
4. Anti noise system according to any of the preceding claims, wherein said system is arranged to perform a frequency dependent weighing of said

error signals (**v**) to yield resulting error signals (**e**) used to control said adaptive filter.

5. Anti noise system according to any of the preceding claims, wherein said system is arranged to perform all calculations in a time domain.

6. Anti noise system according to any of the preceding claims, wherein said system is arranged to weigh said sensor output signals (**q**) with radiation mode shapes (**E**) that are efficient radiators in a first, predetermined frequency band, and to weigh secondary sensor signals ($\mathbf{q}_s$) related to the one or more secondary sources (3a) with further radiation mode shapes (**E'**) that are inefficient radiators in said first frequency band but efficient radiators in a second, predetermined other frequency band.

7. Anti noise system according to any of the preceding claims, wherein said one or more secondary sources comprises a baffled radiator.

8. Anti noise system according to any of the preceding claims, wherein said oneor more secondary sources comprises piezo electric patch actuators on an object.

9. Anti noise system according to any of the preceding claims, wherein said system comprises further sensors in a far field relative to said one or more secondary sources (3a).

10. An anti noise method for suppressing primary signals in a space due to a primary source, comprising the steps of:

- producing secondary signals by one or more secondary sources (3a) to suppress said primary signals in said space;
- producing sensor output signals (**q**) in relation to said secondary sources (3a) by one or more sensors (3b);
- performing the following steps by a controller:
  - receiving said sensor output signals (**q**);

– calculating error signals (**v**) by weighing said sensor output signals (**q**) with radiation mode shapes (**E**) determined for at least one predetermined frequency;

– using said error signals (**v**) to control an adaptive filter to produce drive signals (**u**) for said secondary sources (3a);

wherein said method also performs the following step by said controller (5):

– calculating said error signals (**v**) by weighing said sensor output signals (**q**) with radiation mode shapes (**E**) determined for a plurality of frequencies in a predetermined frequency band.

11. Computer program product to be loaded by an anti noise system for suppressing primary signals in a space due to a primary source, the system comprising:

- one or more secondary sources (3a) to produce secondary signals to suppress said primary signals in said space;
- one or more sensors (3b) to produce sensor output signals (q) in relation to said secondary sources (3a);
- a controller;

the computer program product, after being loaded, providing said controller (5) of the anti noise system with the capacity to:

- receive said sensor output signals (**q**);
- calculate error signals (**v**) by weighing said sensor output signals (**q**) with radiation mode shapes (**E**) determined for at least one predetermined frequency;
- use said error signals (**v**) to control an adaptive filter to produce drive signals (**u**) for said secondary sources (3a);

wherein said computer program product, after being loaded, provides said controller (5) also with the capacity to:

- calculate said error signals (**v**) by weighing said sensor output signals (**q**) with radiation mode shapes (**E**) determined for a plurality of frequencies in a predetermined frequency band.

12. A data carrier provided with a computer program product according to claim 11.

13. A method of calibrating an anti noise system according to any of the claims 1 through 9, comprising the steps of:

- driving said one or more secondary sources (3a) with a plurality of different excitation patterns;
- measuring sensor output signals (**q**) and measuring further sensor output signals (**p**) in said space due to said plurality of different excitation patterns;
- applying said sensor output signals (**q**) and said further sensor output signals (**p**) to said controller (5);
- using a time-domain inverse filtering technique by said controller (5) to determine said radiation mode shapes (**E**).

14. A method of calibrating an anti noise system according to any of the claims 1 through 9, comprising the steps of:

- driving one or more volume velocity sources with a known volume velocity in predetermined locations remote from said secondary sources;
- measuring pressure signals due to said volume velocity sources with said sensors on a structure supporting said secondary sources;
- applying the value of said volume velocity and said pressure signals to said controller (5);
- determining the radiation mode shapes (**E**).

15. A method of calibrating an anti noise system according to any of the claims 1 through 9, comprising the steps of:

- driving said one or more secondary sources (3a) with a plurality of different excitation patterns and measuring said sensor output signals (**q**);
- applying said excitation patterns and said sensor output signals to said controller (5);

- driving one or more sources with a known volume velocity in a predetermined location remote from the secondary sources (3a) and measuring output signals of the secondary sources (3a) due to said one or more sources;
- applying the value of said volume velocity and said output signals on the secondary sources to said controller (5);
- using a time-domain inverse filtering technique by said controller (5) to determine said radiation mode shapes (**E**).

16. A method of calibrating an anti noise system according to any of the claims 13 through 15, wherein said method determines radiation mode shapes (**E**) that are efficient radiators in a first, predetermined frequency band, and wherein said method determines further radiation mode shapes (**E'**) that are inefficient radiators in said first frequency band but efficient radiators in a second, predetermined other frequency band.

Fig 1

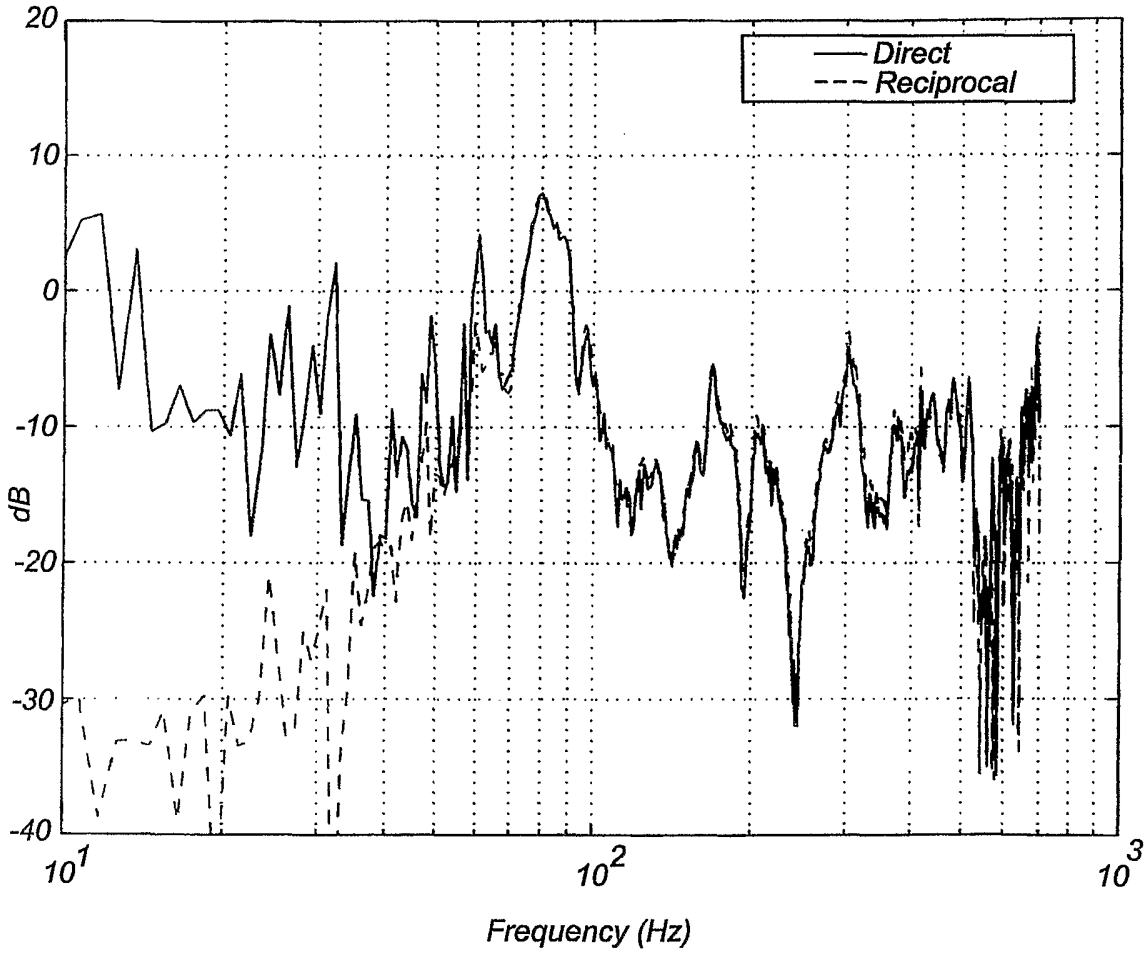
Direct
Reciprocal
20
10
0
-10
-20
-30
-40
dB
10^1
10^2
10^3
Frequency (Hz)

Fig 2a

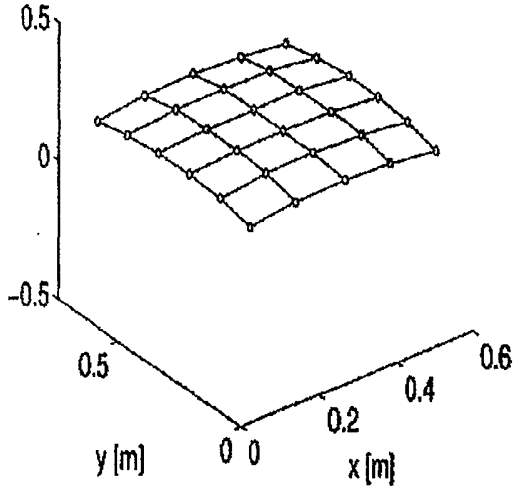

Fig 2b

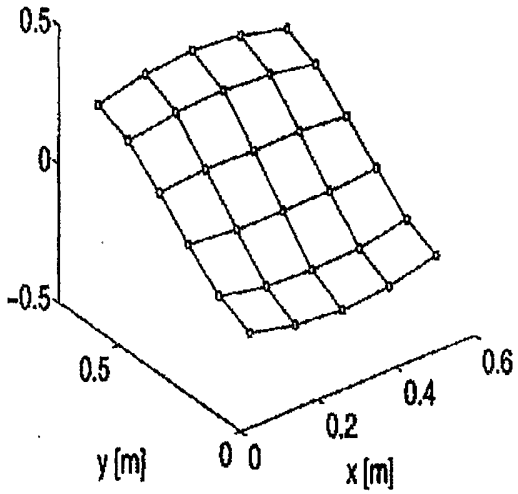

Fig 2c

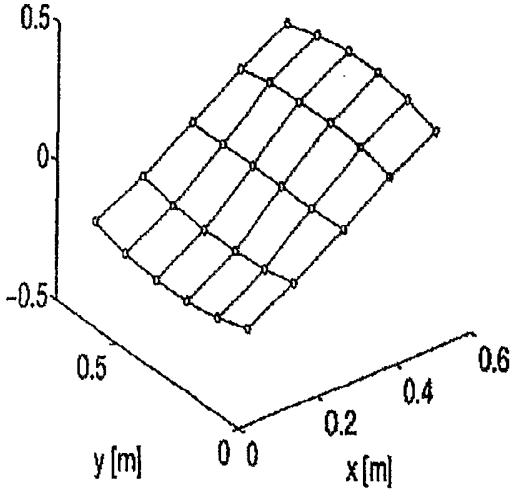

Fig 2d

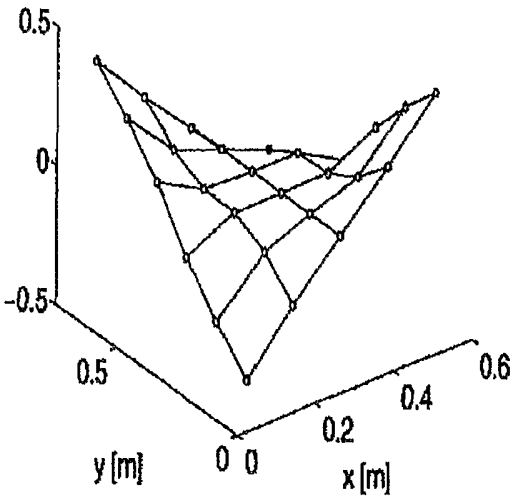

Fig 3

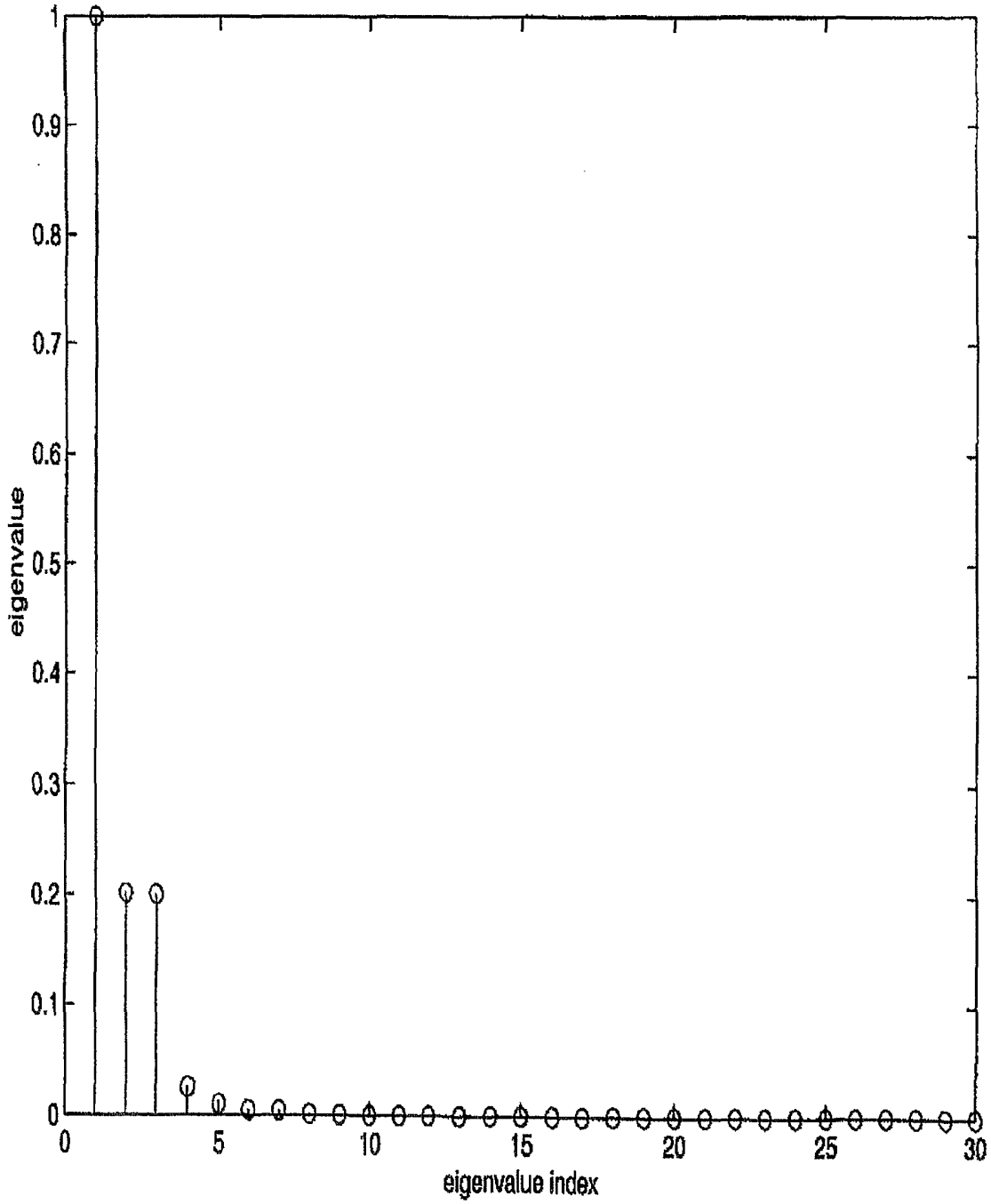
eigenvalue
eigenvalue index
0
0.1
0.2
0.3
0.4
0.5
0.6
0.7
0.8
0.9
1
0
5
10
15
20
25
30

Fig 4a

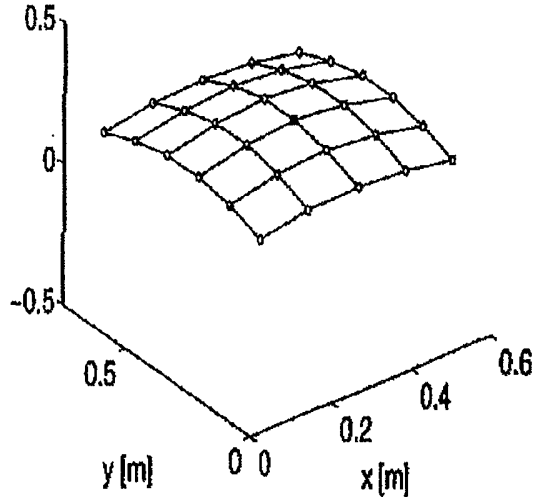

Fig 4b

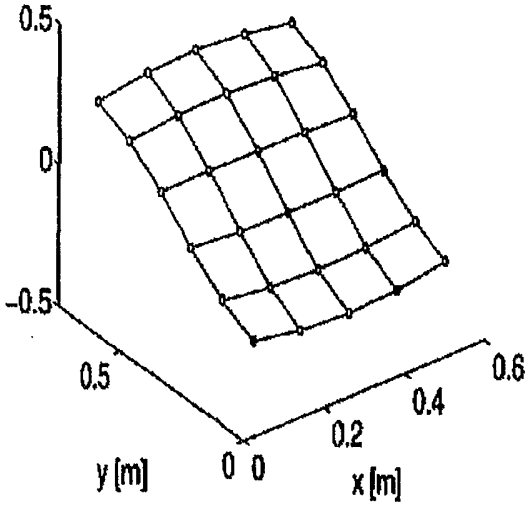

Fig 4c

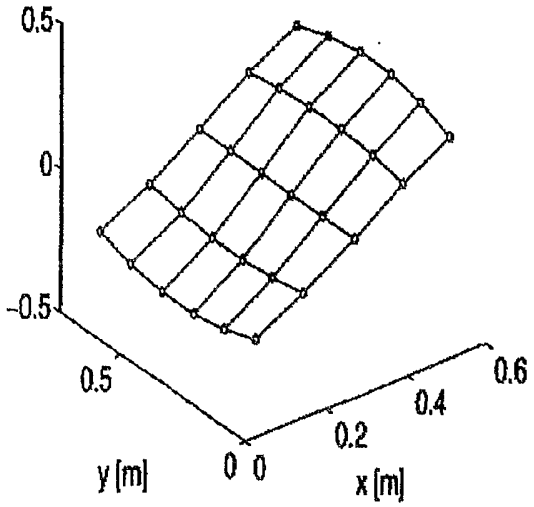

Fig 4d

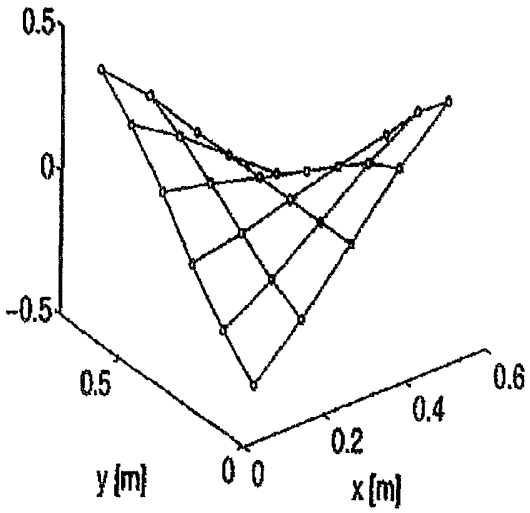

Fig 5

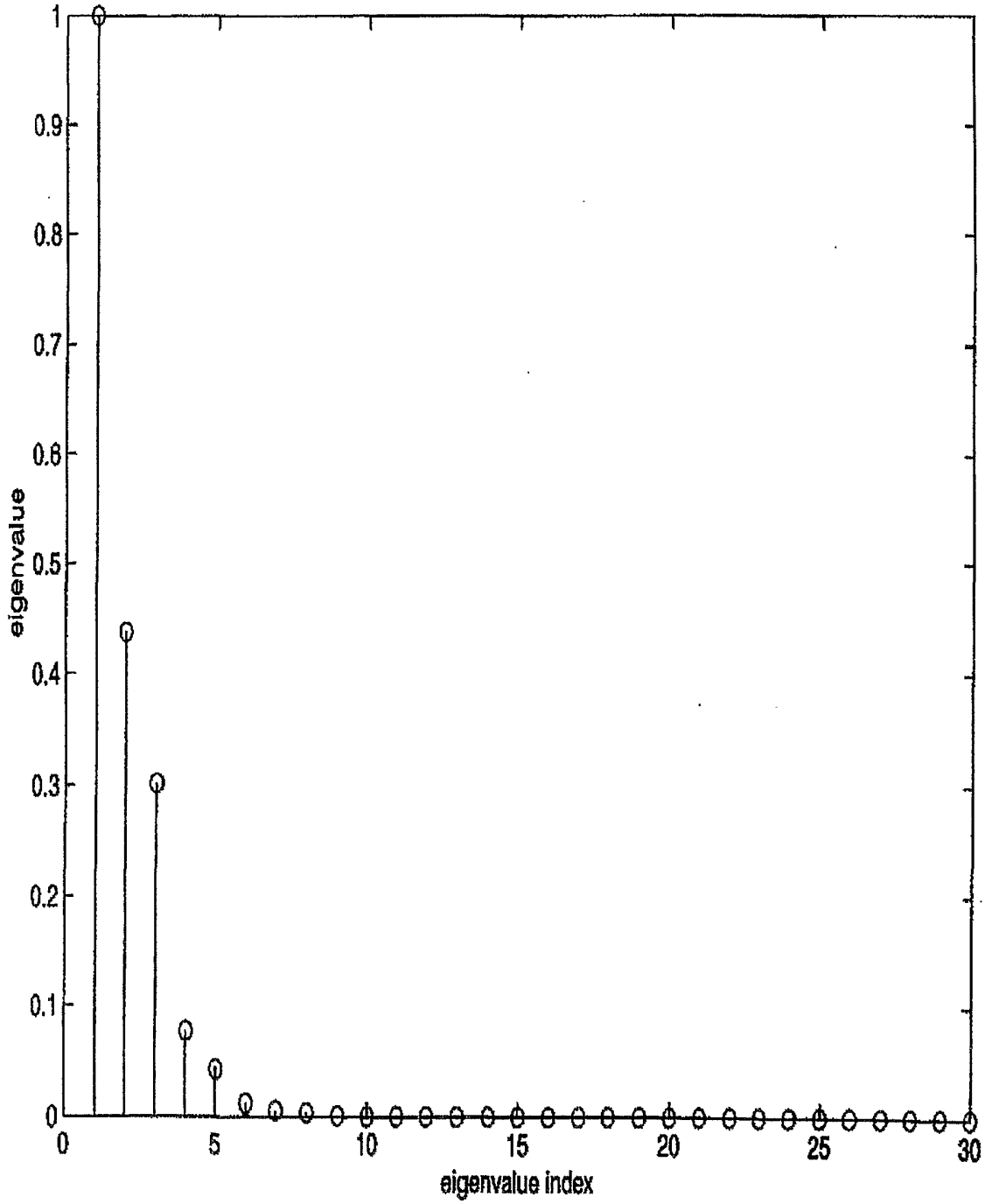
eigenvalue
eigenvalue index
0
0.1
0.2
0.3
0.4
0.5
0.6
0.7
0.8
0.9
1
0
5
10
15
20
25
30

Fig 6a

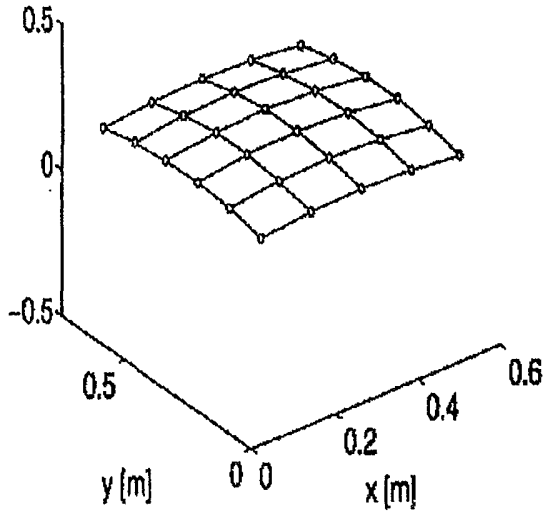

Fig 6b

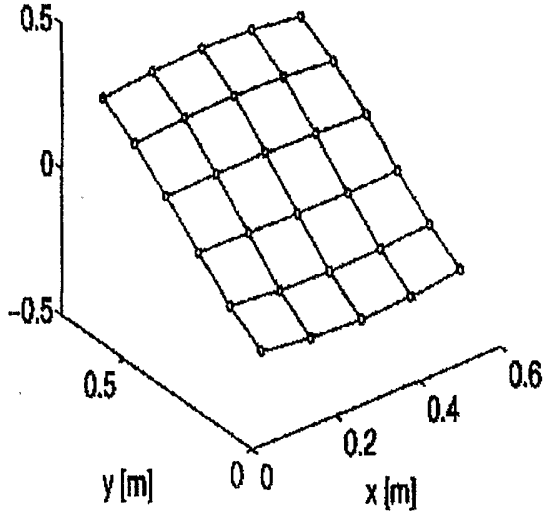

Fig 6c

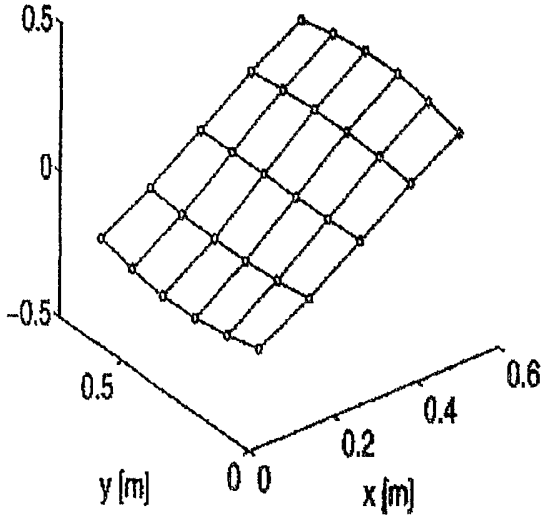

Fig 6d

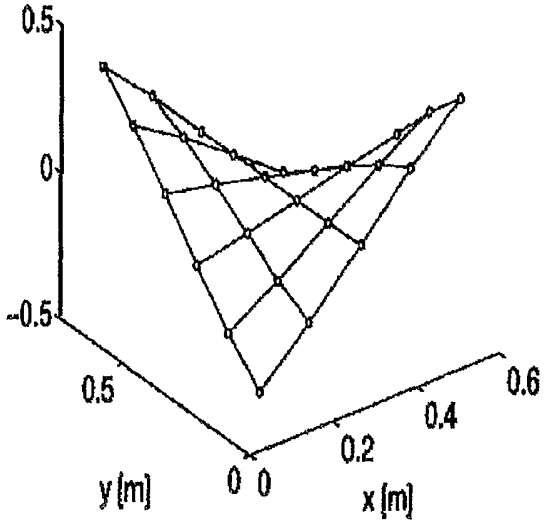

Fig 7

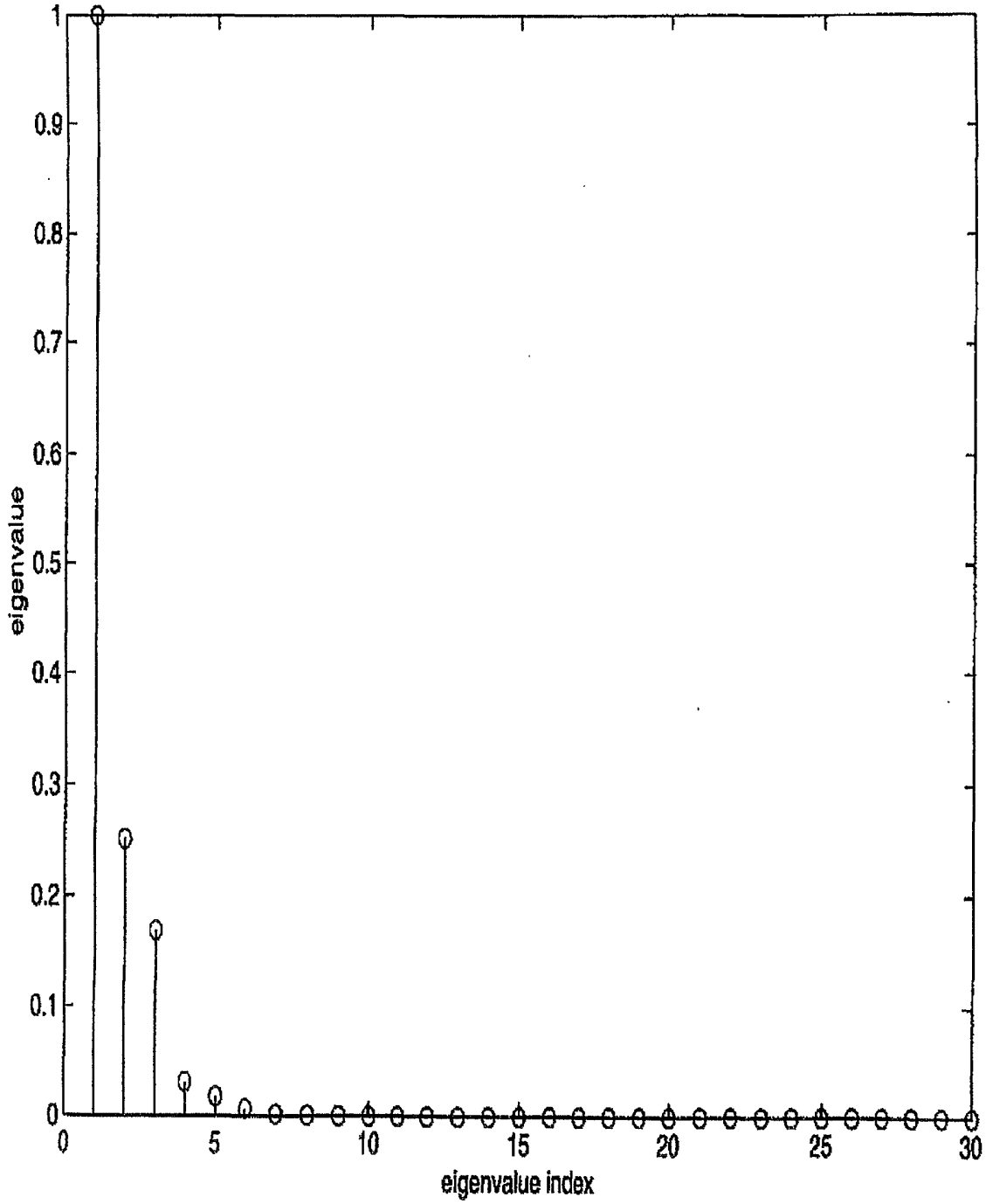
eigenvalue
eigenvalue index
0
0.1
0.2
0.3
0.4
0.5
0.6
0.7
0.8
0.9
1
0
5
10
15
20
25
30

Fig 7

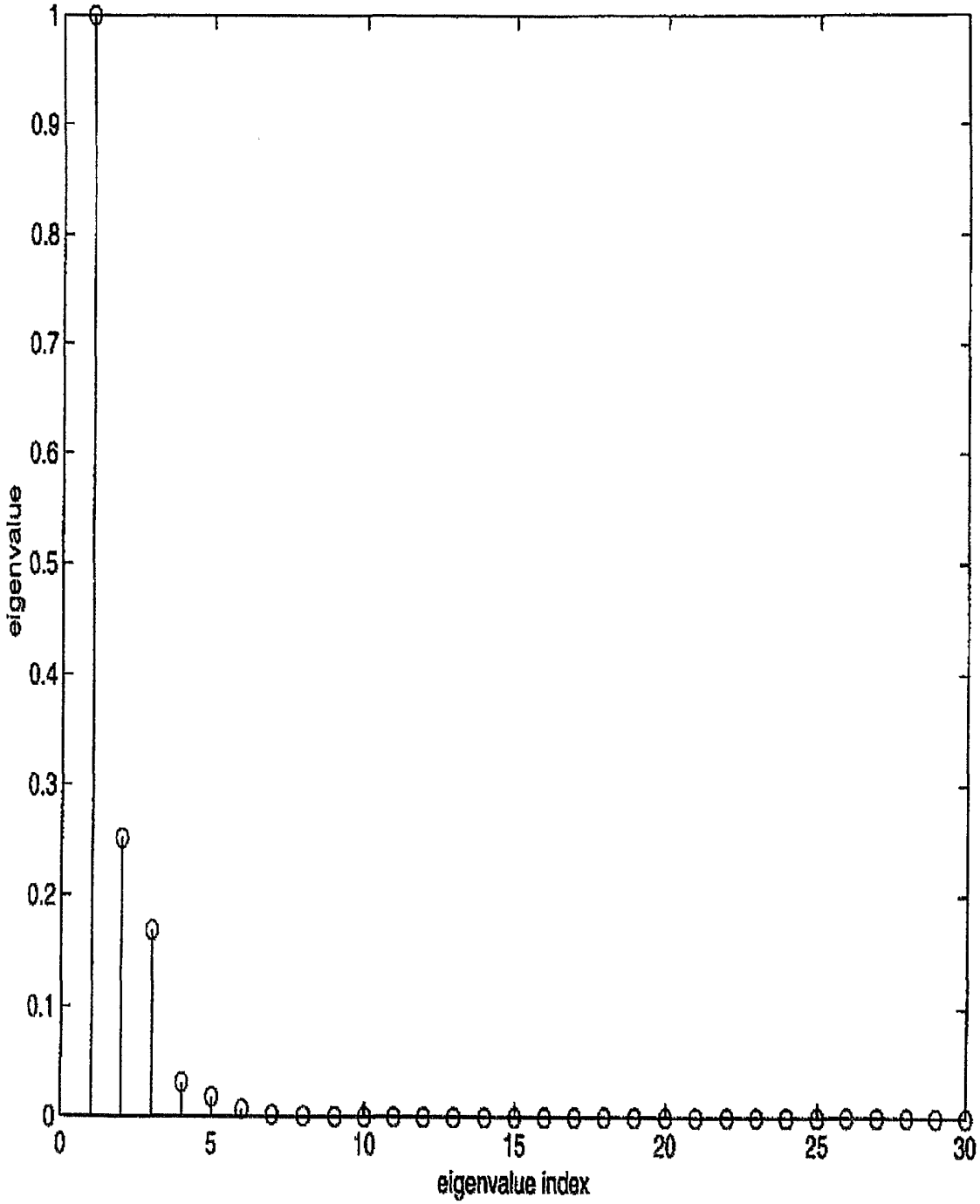
eigenvalue
eigenvalue index
0
0.1
0.2
0.3
0.4
0.5
0.6
0.7
0.8
0.9
1
0
5
10
15
20
25
30

Fig 8a

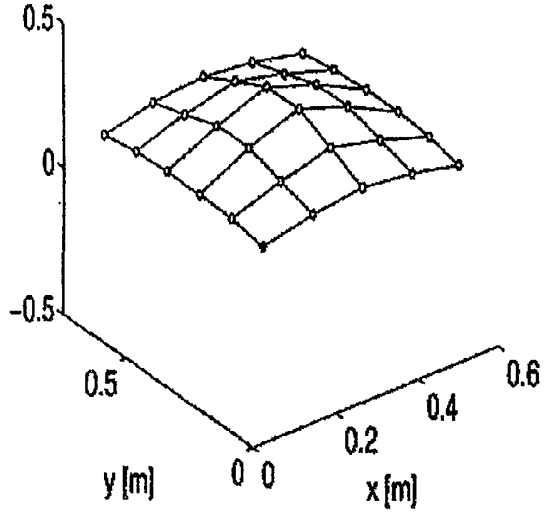

Fig 8b

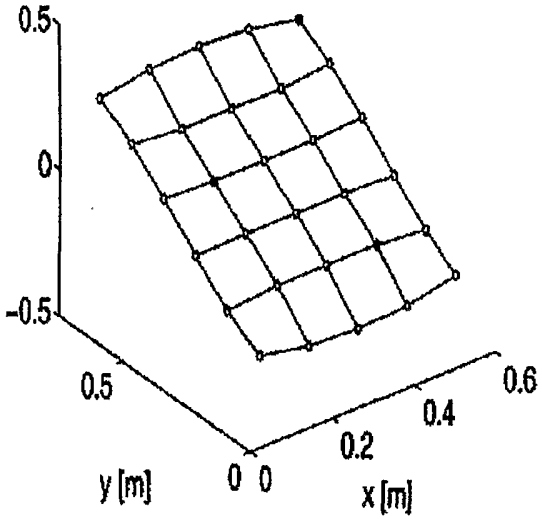

Fig 8c

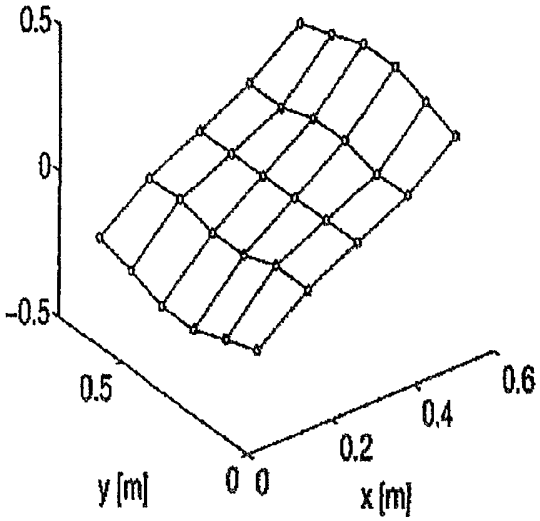

Fig 8d

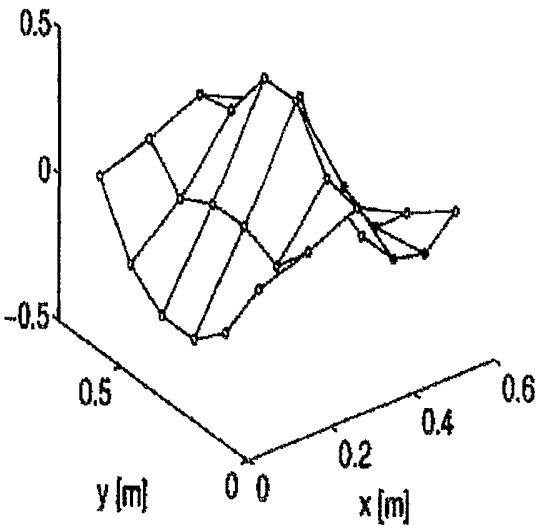

Fig 9

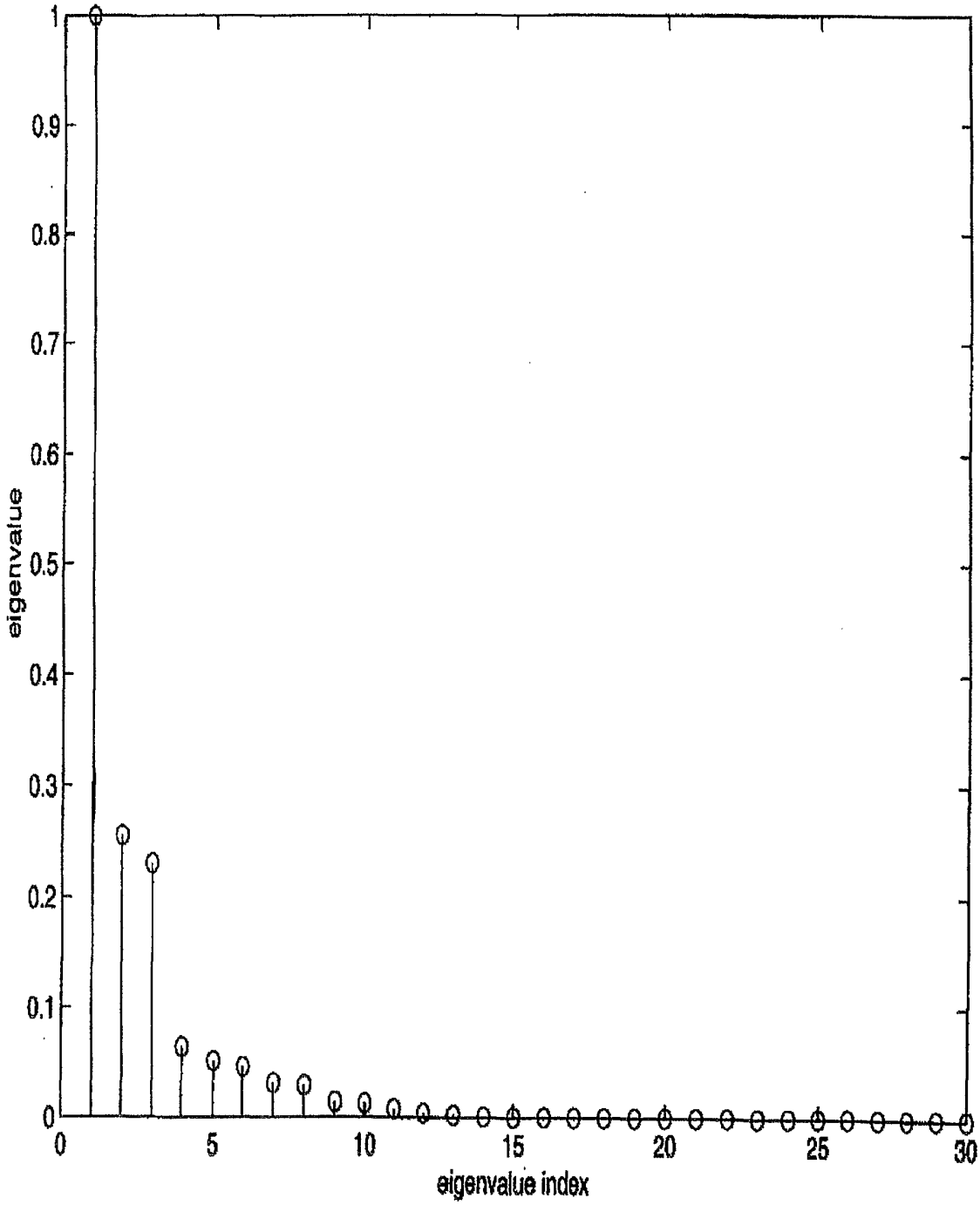
eigenvalue
eigenvalue index
0
0.1
0.2
0.3
0.4
0.5
0.6
0.7
0.8
0.9
1
0
5
10
15
20
25
30

Fig 10

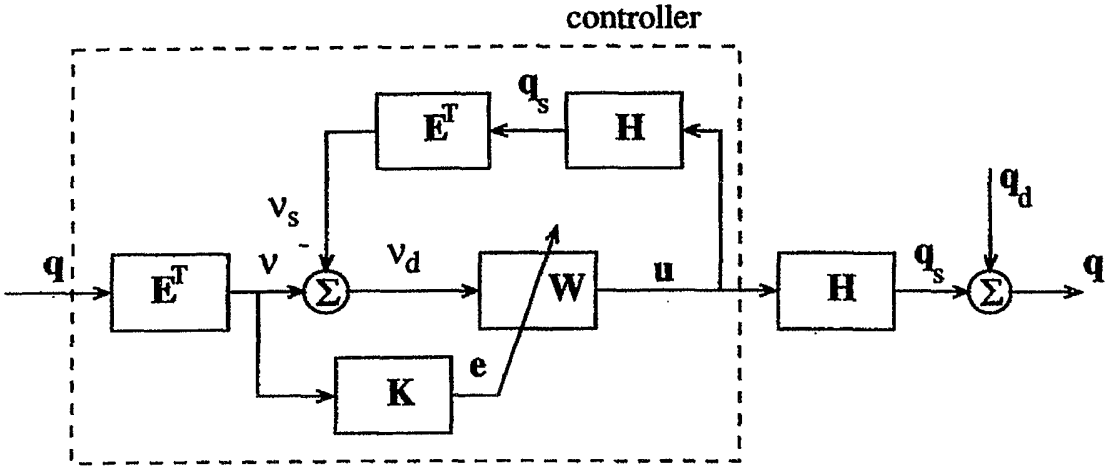

Fig 11a

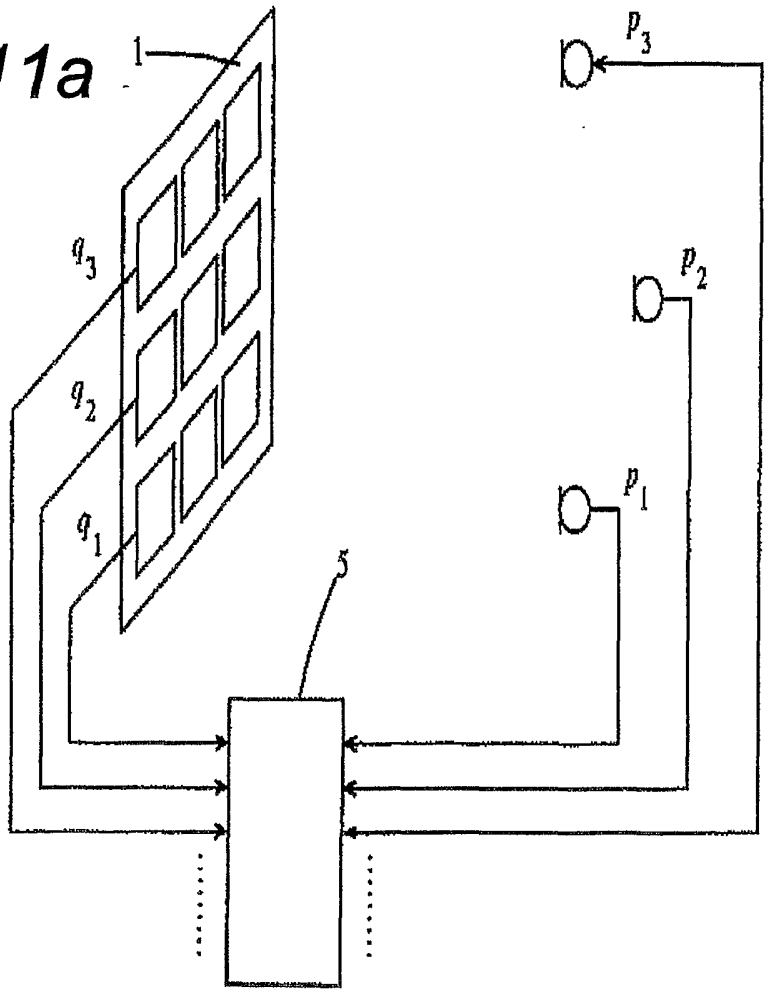

Fig 11b

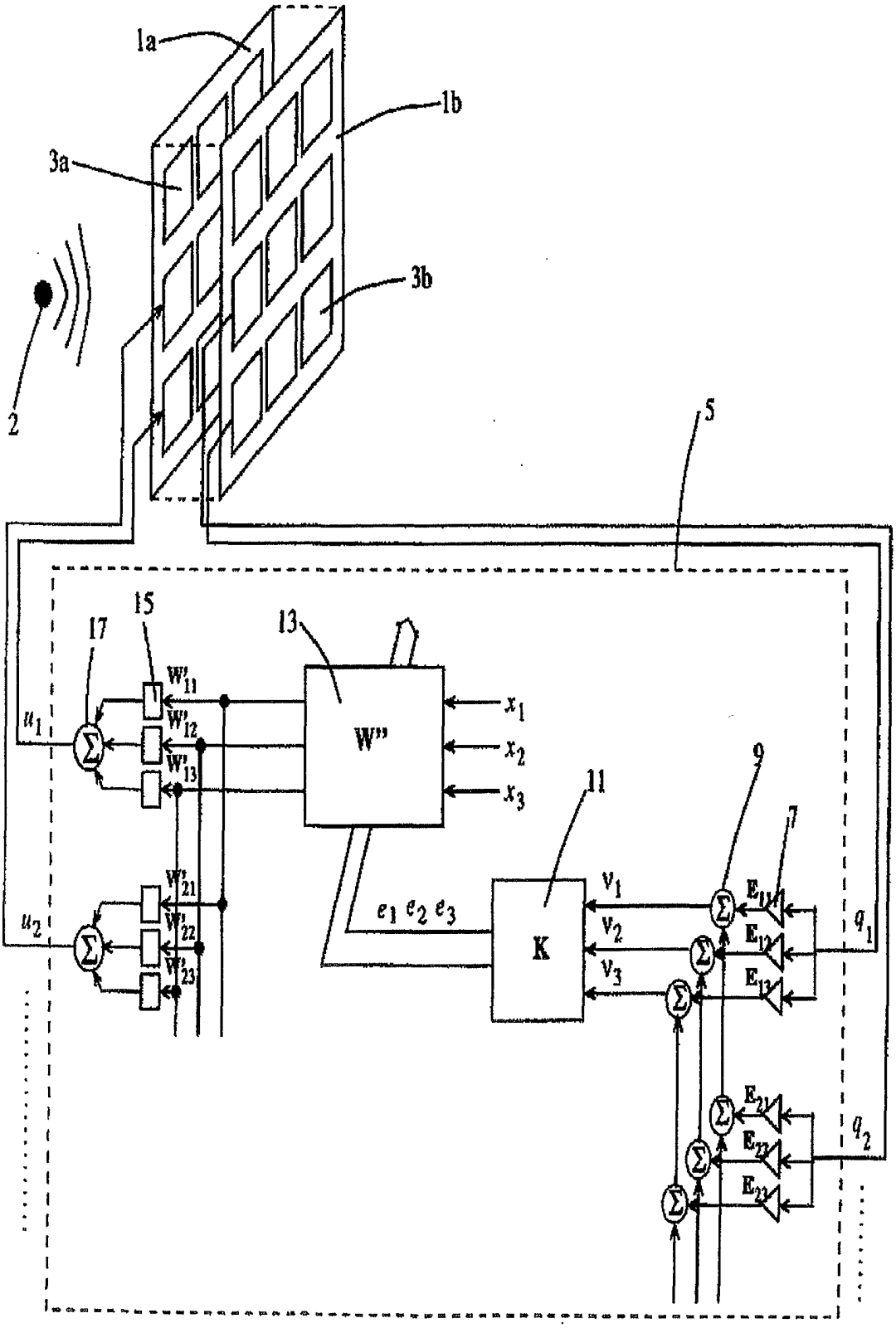

Fig 12

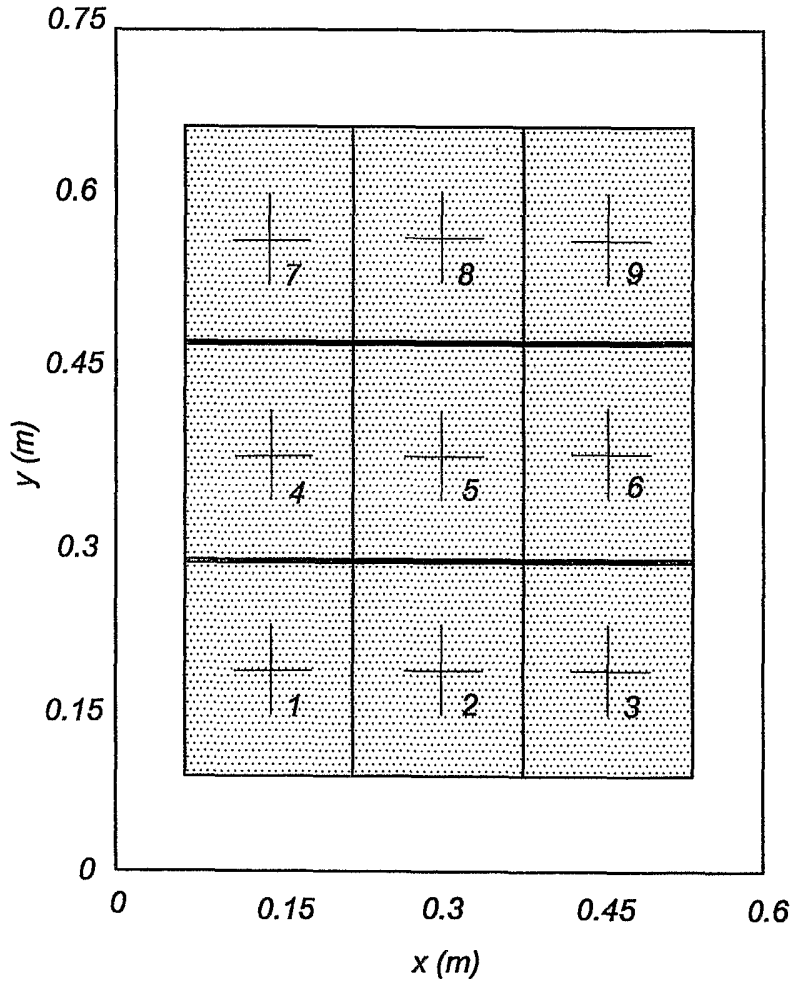

Fig 13

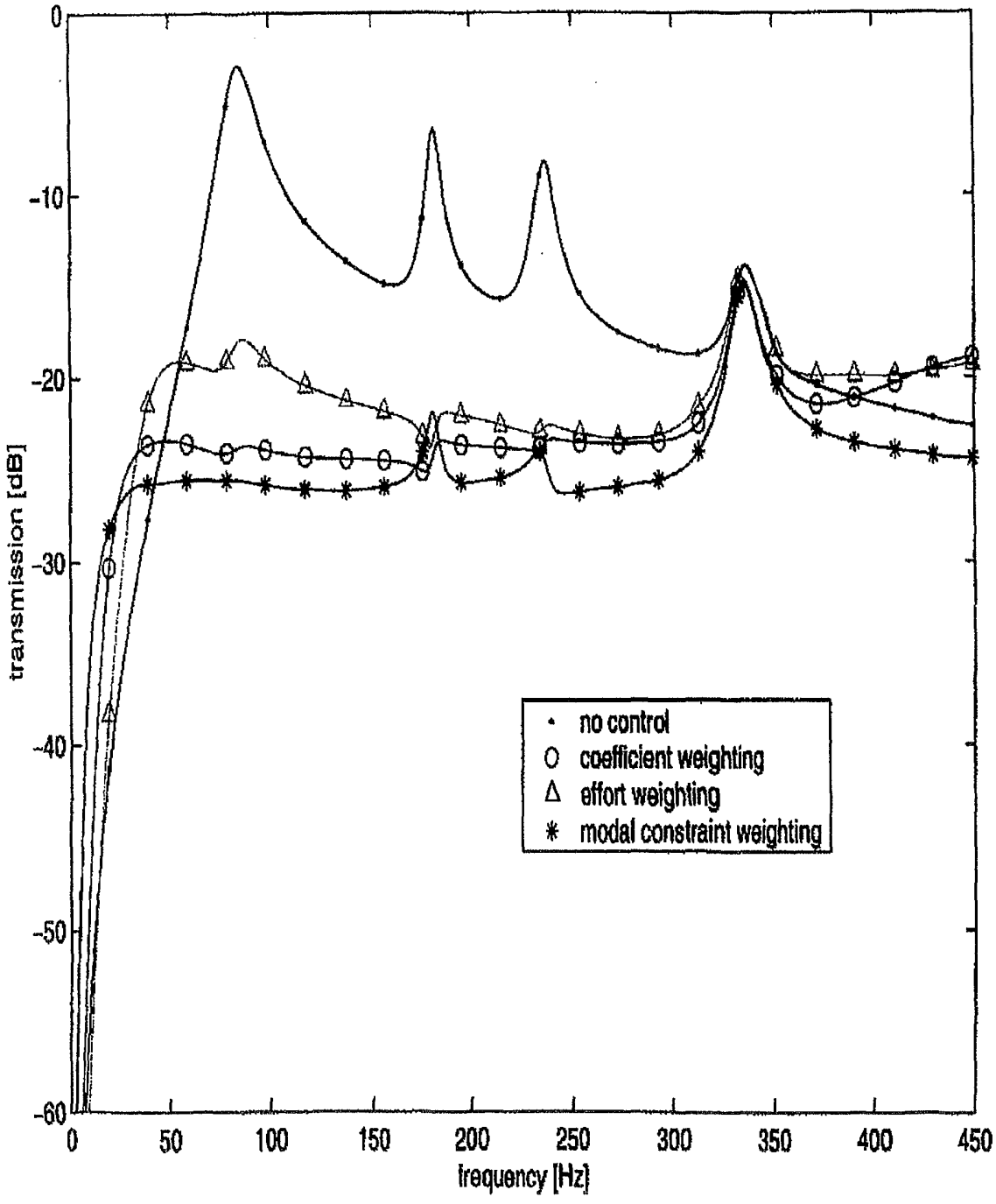
0
-10
-20
-30
-40
-50
-60
transmission [dB]
0
50
100
150
200
250
300
350
400
450
frequency [Hz]
no control
coefficient weighting
effort weighting
modal constraint weighting

INTERNATIONAL SEARCH REPORT

rnational Application No
PCT/NL 02/00297

A. CLASSIFICATION OF SUBJECT MATTER
IPC 7 G10K11/178

According to International Patent Classification (IPC) or to both national classification and IPC

B. FIELDS SEARCHED

Minimum documentation searched (classification system followed by classification symbols)
IPC 7 G10K

Documentation searched other than minimum documentation to the extent that such documents are included in the fields searched

Electronic data base consulted during the international search (name of data base and, where practical, search terms used)
INSPEC, EPO-Internal, WPI Data

C. DOCUMENTS CONSIDERED TO BE RELEVANT

Category °	Citation of document, with indication, where appropriate, of the relevant passages	Relevant to claim No.
Y	US 5 519 637 A (MATHUR GOPAL) 21 May 1996 (1996-05-21) column 2, line 66 -column 3, line 63 ---	1,2,4-8, 10-12
Y	GIBBS G P ET AL: "Radiation modal expansion: Application to active structural acoustic control" JOURNAL OF THE ACOUSTICAL SOCIETY OF AMERICA, JAN. 2000, ACOUST. SOC. AMERICA THROUGH AIP, USA, vol. 107, no. 1, pages 332-339, XP001052698 ISSN: 0001-4966 cited in the application page 334 -page 337 --- -/--	1,2,4-8, 10-12

[X] Further documents are listed in the continuation of box C.

[X] Patent family members are listed in annex.

° Special categories of cited documents :

"A" document defining the general state of the art which is not considered to be of particular relevance

"E" earlier document but published on or after the international filing date

"L" document which may throw doubts on priority claim(s) or which is cited to establish the publication date of another citation or other special reason (as specified)

"O" document referring to an oral disclosure, use, exhibition or other means

"P" document published prior to the international filing date but later than the priority date claimed

"T" later document published after the international filing date or priority date and not in conflict with the application but cited to understand the principle or theory underlying the invention

"X" document of particular relevance; the claimed invention cannot be considered novel or cannot be considered to involve an inventive step when the document is taken alone

"Y" document of particular relevance; the claimed invention cannot be considered to involve an inventive step when the document is combined with one or more other such documents, such combination being obvious to a person skilled in the art.

"&" document member of the same patent family

Date of the actual completion of the international search	Date of mailing of the international search report
11 September 2002	18/09/2002

Name and mailing address of the ISA	Authorized officer
European Patent Office, P.B. 5818 Patentlaan 2 NL – 2280 HV Rijswijk Tel. (+31-70) 340-2040, Tx. 31 651 epo nl, Fax: (+31-70) 340-3016	Swartjes, H

Form PCT/ISA/210 (second sheet) (July 1992)

INTERNATIONAL SEARCH REPORT

ational Application No
PCT/NL 02/00297

C.(Continuation) DOCUMENTS CONSIDERED TO BE RELEVANT

Category °	Citation of document, with indication,where appropriate, of the relevant passages	Relevant to claim No.
A	US 5 315 661 A (GOSSMAN WILLIAM ET AL) 24 May 1994 (1994-05-24) column 5, line 47 -column 6, line 15 ---	1,2,7,8, 10-12
A	US 5 719 945 A (LIANG CHEN ET AL) 17 February 1998 (1998-02-17) column 13, line 3764 ---	1,2,7,8, 10-12
A	PAN X ET AL: "Active control of sound transmission through a double-leaf partition by volume velocity cancellation" JOURNAL OF THE ACOUSTICAL SOCIETY OF AMERICA, NOV. 1998, ACOUST. SOC. AMERICA THROUGH AIP, USA, vol. 104, no. 5, pages 2828-2835, XP001058137 ISSN: 0001-4966 page 2832, right-hand column -page 2834, left-hand column ---	1,2,6,7
A	EP 0 568 282 A (WESTINGHOUSE ELECTRIC CORP) 3 November 1993 (1993-11-03) page 1, line 36 -page 2, line 21 -----	1,9

INTERNATIONAL SEARCH REPORT

Information on patent family members

ational Application No
PCT/NL 02/00297

Patent document cited in search report	Publication date	Patent family member(s)	Publication date
US 5519637 A	21-05-1996	NONE	
US 5315661 A	24-05-1994	AT 194040 T	15-07-2000
		CA 2142013 A1	03-03-1994
		DE 69231190 D1	27-07-2000
		DE 69231190 T2	22-03-2001
		EP 0657058 A1	14-06-1995
		JP 8500193 T	09-01-1996
		WO 9405005 A1	03-03-1994
US 5719945 A	17-02-1998	EP 0713378 A1	29-05-1996
		JP 3027824 B2	04-04-2000
		JP 8508111 T	27-08-1996
		WO 9505136 A1	23-02-1995
EP 0568282 A	03-11-1993	US 5347586 A	13-09-1994
		CA 2094984 A1	29-10-1993
		EP 0568282 A2	03-11-1993
		JP 6043886 A	18-02-1994